

In silico tool for identification of colorectal cancer from cell-free DNA biomarkers

Kartavya Mathur^{1,2}, Shipra Jain¹, Nisha Bajiya¹, Nishant Kumar¹, Gajendra P. S. Raghava *¹

1. Department of Computational Biology, Indraprastha Institute of Information Technology, Okhla Phase
3, New Delhi-110020, India.

2. School of Biotechnology, Gautam Buddha University, Gautam Buddha Nagar, Greater Noida, Uttar
Pradesh, 201308

Mailing Address of Authors

Kartavya Mathur (KM): 221pbg002@gbu.ac.in ORCID ID: <https://orcid.org/0000-0003-3563-5666>

Shipra Jain: shipra@iiitd.ac.in ORCID ID: <https://orcid.org/0000-0002-7045-5188>

Nishant Kumar (NK): nishantk@iiitd.ac.in ORCID ID: <https://orcid.org/0000-0001-7781-9602>

Nisha Bajiya (NB): nishab@iiitd.ac.in ORCID ID: <https://orcid.org/0000-0002-5075-5386>

Gajendra P. S. Raghava (GPSR): raghava@iiitd.ac.in ORCID ID: <https://orcid.org/0000-0002-8902-2876>

***Corresponding Author**

Prof. Gajendra P. S. Raghava

Head and Professor

Department of Computational Biology

Indraprastha Institute of Information Technology, Delhi

Okhla Industrial Estate, Phase III (Near Govind Puri Metro Station)

New Delhi, India – 110020 Office: A-302 (R&D Block)

Phone: 011-26907444

Email: raghava@iiitd.ac.in

Website: <http://webs.iiitd.edu.in/raghava/>

1. Abstract

Colorectal cancer (CRC) remains a major global health concern, with early detection being pivotal for improving patient outcomes. In this study, we leveraged high-throughput methylation profiling of cell-free DNA (cfDNA) to identify and validate diagnostic biomarkers for CRC. The GSE124600 study data were downloaded from the Gene Expression Omnibus (GEO), as the discovery cohort, comprising 142 CRC and 132 normal cfDNA methylation profiles obtained via MCTA-seq. After preprocessing and filtering, 97,863 CpG sites were retained for further analysis. Differential methylation analysis using statistical tests identified 30,791 CpG sites as significantly altered in CRC samples ($p < 0.05$). Univariate scoring enabled the selection of top-ranking features, which were further refined using multiple feature selection algorithms, including Recursive Feature Elimination (RFE), Sequential Feature Selection (SFS), and SVC-L1. Various machine learning (ML) models—such as Logistic Regression, Support Vector Machines, Random Forest, and Multi-layer Perceptron—were trained and tested using independent validation datasets. The best performance was achieved with an MLP model trained on 25 features selected by RFE, reaching an AUROC of 0.89 and MCC of 0.78 on validation data. Additionally, a deep learning-based convolutional neural network (CNN) achieved an AUROC of 0.78. Functional annotation of the most predictive CpG sites identified several genes involved in key cellular processes, some of which were validated for differential expression in CRC using the GEPIA2 platform. Our study highlights the potential of cfDNA methylation markers combined with ML/DL models for non-invasive and accurate CRC detection, paving the way for clinically relevant diagnostic tools.

Author's Biography

1. Kartavya Mathur is currently studying as an M.Sc. student at Gautam Buddha University, Greater Noida, Uttar Pradesh, India. He is currently working as an Intern on a Project position at the Department of Computational Biology, Indraprastha Institute of Information Technology (IIIT), New Delhi, India.
2. Shipra Jain is currently working as Ph.D. in Computational Biology from the Department of Computational Biology, Indraprastha Institute of Information Technology, New Delhi, India.

3. Nisha Bajiya is currently working as Ph.D. in Computational Biology from the Department of Computational Biology, Indraprastha Institute of Information Technology, New Delhi, India.
4. Nishant Kumar is currently working as Ph.D. in Computational Biology from the Department of Computational Biology, Indraprastha Institute of Information Technology, New Delhi, India.
5. Gajendra P. S. Raghava is currently working as Professor and Head of the Department of Computational Biology, Indraprastha Institute of Information Technology, New Delhi, India.

Abbreviations

AB: AdaBoost

AUROC: Area Under the Receiver Operating Characteristics

Acc: Accuracy

CEA: Carcinoembryonic Antigen

CNN: Convolutional Neural Network

CRC: Colorectal carcinogenesis

DT: Decision Tree

ET: Extra Trees Classifier

GB: Gradient Boosting

GEO: Gene Expression Omnibus

KN: K-Nearest Neighbor

LR: Logistic Regression

MCC: Matthews Correlation Coefficient

MLP: Multi-Layer Perceptron

NB: Naïve Bayes

RF: Random Forest

RFE: Recursive Feature Elimination

Sens: Sensitivity

SFS: Sequential Feature Selector

Spec: Specificity

SVC: Support Vector Classifier

2. Introduction

Colorectal carcinogenesis (CRC), arising due to abnormal growth of cells lining the colon and rectum regions of the large intestine, has become one of the most frequent malignancies globally [1,2]. According to the GLOBOCAN 2022 survey by Global Cancer Observatory (<https://gco.iarc.fr/en>), colorectal cancer is the third most common carcinoma globally in terms of incidence, with an Age-Standardized Rate (ASR) of 18.4 per 100,000 and mortality and ranks second most deadliest among all cancer types with 5.7 million prevalent cases in a span of 5-years [3]. According to cancer statistics published in the Cancer Journal for Clinicians, the United States alone accounts for nearly 152,810 cases of CRC, with an estimated death of nearly 53,010 [4]. Among the highest colorectal cancer incidence countries in 2022, India ranks sixth in terms of incidence (n = 70,038) and mortality (n = 40,993) (<https://www.wcrf.org/preventing-cancer/cancer-statistics/colorectal-cancer-statistics/>). These statistics emphasize the importance of early detection of CRC to reduce morbidity and mortality. Early recognition of CRC is challenging as there are very limited clinical symptoms, therefore, the majority of cases are identified at progressive stages when radical action is no longer a viable option.

Colorectal cancer (CRC) testing involves a spectrum of screening, diagnostic, and biomarker evaluations available in the market [5,6]. Standard screening methods include Fecal Occult Blood Tests (FOBT) and the Fecal Immunochemical Test (FIT), which detect hidden blood in stool but may miss polyps or cancers that do not bleed consistently [7–9]. Stool DNA tests detect genetic level changes but are costly and less accessible in small labs [10,11]. Colonoscopy is the cornerstone examination recommended by medical practitioners, which enables direct visualization, biopsy, and polyp removal, but it is an invasive procedure and carries risks like perforation of the intestine [12–14]. CT colonography and flexible sigmoidoscopy are less invasive but cannot detect small polyps developed in the initial stage and may require follow-up colonoscopy in case of abnormalities [15–18]. Blood tests such as Carcinoembryonic Antigen (CEA) and Carbohydrate Antigen (CA-19) are also widely used for monitoring but lack sensitivity and specificity for early detection [19–22]. CEA sensitivity in CRC varies from 65 to 74%, while CA19-9 sensitivity ranges between 26% and 48%. However, together, they provide

an increased specificity and sensitivity [23]. A recent study found that patients with CEA or CA19-9 levels exceeding 200 had a lower 5-year overall survival (OS) than those below 200 or within the normal range. Additionally, individuals with elevated levels of both markers experienced a significantly shorter 5-year OS [24]. Recently, detecting methylated SEPT9 (mSEPT9) in blood has gained attention as a valuable tool for CRC screening. An enhanced mSEPT9 test demonstrated an overall recall of 90% and a specificity of 88% [25,26]. Despite the significant advancements made in analyzing genomic, transcriptomic and epigenomic profiles of colorectal cancer patients, we still lack specific biomarkers.

With recent advancements in genomic and transcriptomic profiling, liquid biopsies have emerged as a minimally invasive alternative and have appeared promising for detecting circulating biomarkers in body fluids, especially blood. Epigenetic modifications, including methylation and histone alterations, and non-coding RNAs like long noncoding RNAs (lncRNAs) and microRNAs (miRNAs) expressed during early carcinogenesis have been suggested as highly specific indicators of cancer presence and progression [27]. DNA methylation, in particular, plays an essential role in modulating gene expression and, therefore, is dysregulated in cancer cells [28]. Aberrant methylation patterns in circulating tumor DNA (ctDNA) from liquid biopsies (or cell-free DNA) can be used to monitor disease states as well as distinguish between cancerous and normal samples [29,30]. Molecular and genetic testing, including KRAS, NRAS, and BRAF mutations and Microsatellite Instability (MSI), shows highly specific personalized treatment but may not be universally accessible and can have high costs [31–33]. Tailored testing strategies are the need of the hour, which can optimize CRC prevention, early detection, and proper disease management.

Over the years, machine learning (ML) has emerged as a powerful tool in cancer diagnostics. ML techniques can analyze high-dimensional data generated by liquid biopsy methods, allowing for identifying patterns and genetic alterations that traditional methods might overlook. ML-based in-silico prediction tools can detect cancer before symptoms and reduce the risk of invasive procedures like repeated biopsies. These techniques hold immense promise in improving diagnostic accuracy, personalizing treatment strategies, and reducing the reliance on invasive procedures. In the present study, we aimed to develop a robust ML classifier capable of distinguishing between normal and colorectal cancer liquid biopsy samples using epigenomic signatures, specifically focusing on DNA methylation profiles. We hypothesized that ML models

trained on these methylation patterns could achieve high sensitivity and specificity in differentiating cancerous from non-cancerous samples, potentially paving the way for a non-invasive and reliable diagnostic tool for CRC screening. Our approach involved the integration of key steps, including the extraction and processing of DNA methylation data, the selection of informative features, and the training of ML models. We evaluated the performance of various classifiers, optimized their parameters, and validated the results on an independent validation dataset. By leveraging the power of epigenomics and ML, this study seeks to contribute to developing next-generation diagnostic tools for colorectal cancer, focusing on early detection and improved patient outcomes.

3. Methodology

3.1. Data Acquisition

We explored the methylation profiles of Colorectal Cancer (CRC) samples from Gene Expression Omnibus (GEO) using a pre-designed keyword search strategy: “((cell free DNA[All Fields] OR cfDNA[All Fields] OR circulating tumor DNA[All Fields] OR ctDNA[All Fields]) AND (“colorectal neoplasms”[MeSH Terms] OR colorectal cancer[All Fields]) OR CRC[All Fields] OR (colorectal[All Fields] AND (“adenocarcinoma”[MeSH Terms] OR adenocarcinoma[All Fields])) OR (“colorectal neoplasms”[MeSH Terms] OR colorectal carcinoma[All Fields])) AND “Homo sapiens”[porgn]”. The accessions retrieved from the keywords were further filtered based on publication year, availability of processed dataset, and cell-free DNA obtained from blood specimens. The filtered datasets thus obtained were further grouped based on their methodology and ranked according to sample size. An in-house R script was used to download the processed datasets. The datasets were reassessed for sample size, balanced dataset, number of methylation sites and availability of proper annotations. Based on these parameters, GSE124600 was selected as the discovery cohort. We obtained 142 cancerous (CRC) and 132 control (Normal) sample methylation profiles from this dataset. The stage distribution of the cancerous sample of these patients is displayed in Figure 1. The data originated from the methylated CpG tandem amplification (MCTA) sequencing technique, which provided methylated alleles per million mapped reads as a measure for the quantification of gene expression using methylation profiling through high-throughput sequencing.

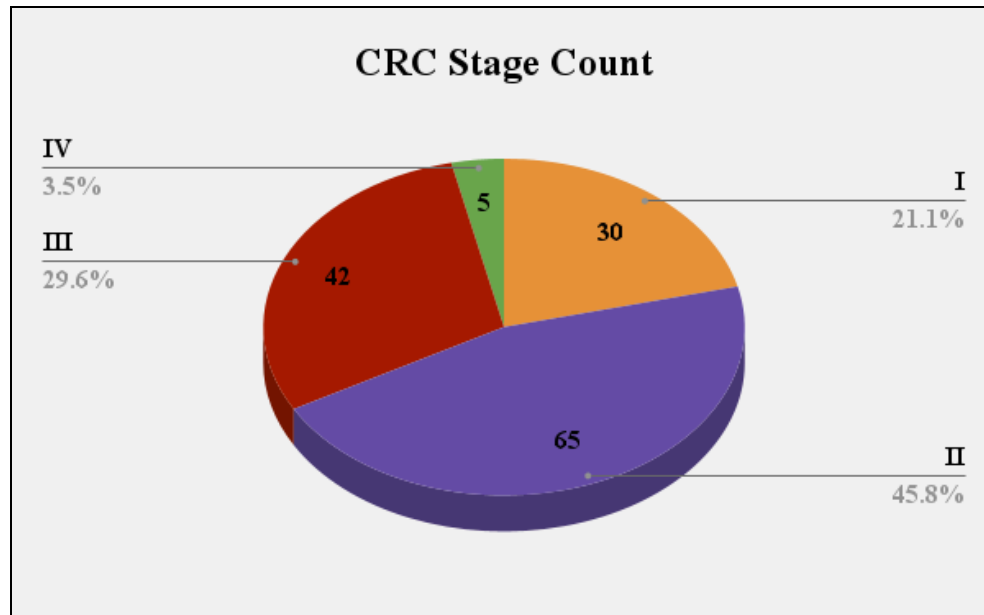


Figure 1: Pie chart showing stage distribution of CRC samples.

3.2. Data Preprocessing

We identified approximately 214,490 CpG methylated sites across the dataset for the cancer and control groups, which were examined for any missing values. The missing values were replaced with '0'. Basic statistical measures were calculated for each methylation site, including mean, standard deviation, and variance. The mean difference was computed to differentiate between cancer and normal samples. Around 54.38% of the sites showed a mean difference of 0 between the two groups, which were excluded from the study using a custom Python script. As a result, the number of CpG sites was reduced to 97,863 for further analysis.

3.3. Identification of differentially methylated CpG sites

We utilized the previously estimated mean methylation scores for each site in cancer and normal samples to identify differentially expressed methylation sites. Following this, a two-tailed independent Student's t-test was performed using a custom Python script to evaluate the statistical significance of the filtered methylation sites based on the mean values of CRC and normal samples. 30791 methylation sites out of 97863 with a confidence level greater than 95% ($p < 0.05$) were considered significant. We performed further analysis on these 30791

differentially methylated sites for the identification of diagnostic biomarker methylation sites, which can screen CRC and control groups with precision.

3.4. Feature Engineering and Feature Selection

Using the univariate score of 30791 sites, methylation sites were differentiated as positively correlated ($U > 0$) and negatively correlated ($U < 0$) among CRC and control samples. Upon that, Area Under Receiver Operating Characteristics (AUROC) based feature engineering was implemented, and single-feature-based models were developed to discriminate between cancerous and non-cancerous samples. The single-feature-based (or threshold-based) model was developed wherein the features with a probability score above the threshold are assigned to the normal class if found upregulated in normal samples, or it is assigned to a colorectal cancer class if upregulated in cancerous samples. Sorting was done based on maximum AUROC, and the top 100 methylation sites for both positive and negative correlation were selected. From the selected 100 methylation sites, sets of 25, 15, and 5 best-performing methylation sites were created for positively and negatively correlated sites to identify the minimal features, which can screen for either group. In addition to this, we have also implemented popular feature selection techniques separately on each positively and negatively correlated sets, like Recursive Feature Selection (RFE), Sequential Feature Selection and SVC-LI-based methods from the scikit-learn package.

3.5. Development of ML and DL based Models

In this study, for training our machine learning based classifier, we deployed eleven different algorithms, including Support Vector Classifier (SVC), Decision Tree (DT), Random Forest (RF), K-Nearest Neighbor (KNN), Logistic Regression (LR), Naïve Bayes (NB), XGBoost, AdaBoost (AB), Gradient Boosting (GB), Extra Trees Classifier (ET), and Multi-Layer Perceptron (MLP). A deep learning-based Convolutional Neural Network (CNN) was also implemented to develop a colorectal cancer diagnostic model.

3.6. Performance Evaluation

In this study, both internal validation via k-fold cross-validation and external validation using an independent dataset were executed to evaluate the models' performance. As depicted in Figure 2, the dataset of a total of 274 samples was randomly split in an 80:20 ratios, where 80% of the data

219 samples (103 healthy and 116 CRC) is allocated for training called as training dataset, and 20% data of 55 samples (29 healthy and 26 CRC) is used for validation called as validation dataset or independent dataset. The training dataset was used to build and evaluate models through a 5-fold cross-validation technique. Model performance on the testing dataset is called internal validation, where parameters are optimized to achieve the best results. To prevent over-optimization, the final model from internal validation (5-fold cross-validation) was further tested on an independent dataset that was not involved in training or testing. Additionally, in the present study, a cross-platform validation was also conducted using data from a different colorectal cancer study, GSE149438.

Both threshold-dependent and threshold-independent parameters were employed to measure the performance of models. In the case of threshold-dependent parameters, we computed sensitivity, specificity, accuracy and Matthew's correlation coefficient (MCC) using the following equations.

$$\text{Sensitivity} = \frac{TP}{TP+FN} * 100 \quad (1)$$

$$\text{Specificity} = \frac{TN}{TN+FP} * 100 \quad (2)$$

$$\text{Accuracy} = \frac{TP+TN}{TP+FP+TN+FN} * 100 \quad (3)$$

$$\text{MCC} = \frac{(TP*TN) - (FP*FN)}{\sqrt{(TP+FP)(TP+FN)(TN+FP)(TN+FN)}} \quad (4)$$

Where FP is false positive, FN is false negative, TP is true positive, and TN is true negative.

For threshold-independent measures, we used the standard parameter Area Under the Receiver Operating Characteristic curve (AUROC). The AUROC curve is generated by plotting sensitivity or true positive rate against the false positive rate (1-specificity) at various thresholds. Finally, the area under the ROC curve is calculated to compute a single AUROC parameter. AUROC with CI (Confidence Interval) were computed using the scikit-learn metrics module.

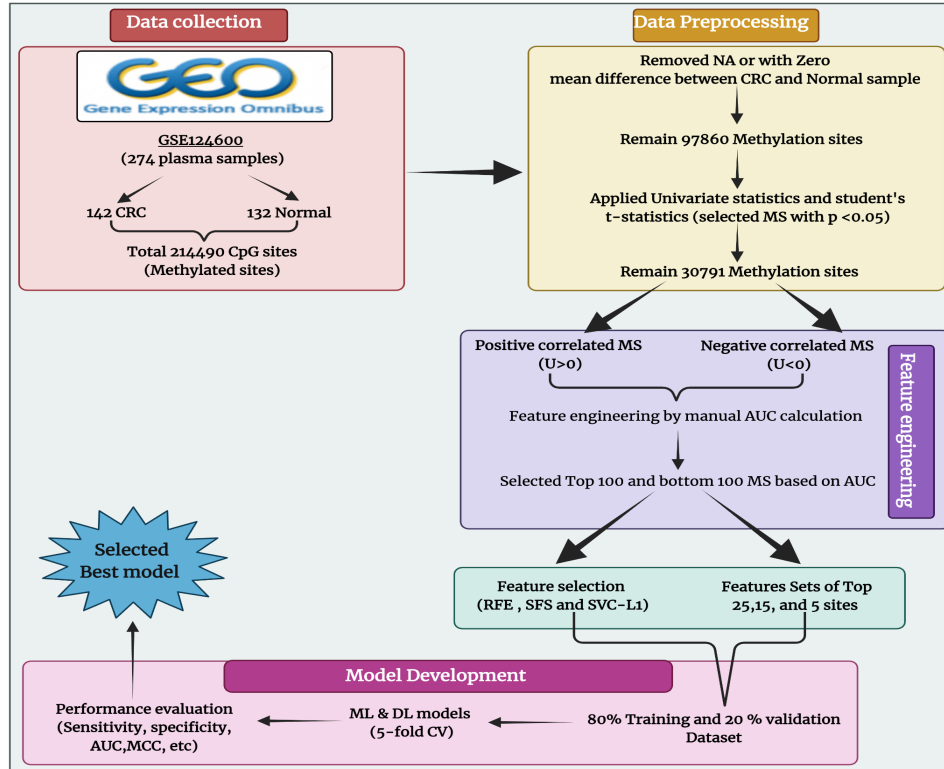


Figure 2: Illustration of the complete study pipeline, providing a detailed stepwise description.

3.7. Functional Annotation and Gene Ontology Analysis

Gene enrichment analysis was conducted using gProfiler to determine the biological significance of genes associated with signature CpG sites. This tool employs the Fisher exact test to compute gene enrichment scores and applies a correction to derive a Z-score. Further to this, the biological functions of relevant genes were retrieved from the GeneCards database for extrapolation. In addition, we have also utilized GEPIA2 tool [34] to validate the expression of our genes in colon and rectum cancers.

4. Results and Discussion

4.1. Preliminary data analysis

4.1.1 Differentially methylated CpG sites:

In the present study, we performed preliminary data statistical analysis by calculating the mean difference of various methylated CpG sites among CRC and control groups. Firstly, we

designated a unique ID to each methylated CpG site, which can be referred to in Supplementary Table 1. Then, we calculated several statistical parameters, such as mean, variance, and standard deviation for each ID for both the cancer and control groups. As evident from Table 1, we observed the highest absolute mean difference among CRC and normal groups is 346.43 for 60881 ID. The statistical analysis parameters for 30791 IDs can be referred to in Supplementary Table 2.

Table 1: List of top 10 significant differential methylation sites based on the highest absolute mean difference.

CpG site ID	Mean_CRC	Mean_NOR	Abs_Mean_Diff
60881	761.17	1107.60	346.43
117819	694.09	963.57	269.49
60882	624.16	891.25	267.08
117820	650.18	888.81	238.62
60883	522.78	742.58	219.80
60884	394.99	571.43	176.45
117848	453.43	628.26	174.83
60885	328.94	474.48	145.55
117829	356.05	488.69	132.64
117830	348.69	473.21	124.51

4.1.2. Univariate analysis

In this study, we screened 30791 significant methylation sites out of 97863 with a confidence level greater than 95% ($p < 0.05$) using their univariate score. Based on univariate statistics, we divided our 30791 significantly enriched methylation sites into positively correlated ($U > 0$) and negatively correlated ($U < 0$) sets and selected the top 100 positively and negatively correlated sites. The top 5 positively and negatively correlated methylated sites are provided in Table 2, while the complete score of each site can be found in Supplementary Table 2. We identified that most of our significantly enriched methylation sites were associated with essential protein-coding genes and non-coding transcripts, which were potentially linked to various cell signaling, developmental, or gene regulatory pathways. The list of the top 5 positively and negatively correlated methylation sites between colorectal cancer and normal samples is depicted in Table 2.

Table 2: List of the top 5 positively and negatively correlated methylation sites between colorectal cancer and normal samples.

Top 5 positively correlated sites				Top 5 negatively correlated sites			
Site ID	Univariate score	t-test score	p-value	Site ID	Univariate score	t-test score	p-value
155365	0.46	5.77	2.17E-08	75318	-0.37	-6.09	3.80E-09
155366	0.46	5.74	2.57E-08	75319	-0.37	-6.11	3.39E-09
162112	0.46	6.08	4.02E-09	7576	-0.37	-5.99	6.53E-09
162111	0.45	6.02	5.64E-09	7575	-0.37	-5.99	6.64E-09
197621	0.45	5.32	2.18E-07	7574	-0.39	-6.29	1.26E-09

4.2. Performance of Machine learning models

4.2.1. Single feature-based ML performance:

In the present study, we developed single-feature-based machine learning models based on the mean score of two groups, i.e. cancer and control groups. In order to implement a single feature-based model, we choose the top 100 positively and 100 negatively correlated methylated sites of 30791 sites. The performance parameters for 200 sites can be referred in Supplementary Table 3. We reported the highest AUROC as 0.75 for positively correlated site “181489” and 0.67 for negatively correlated site “3658”, respectively.

4.2.2. ML model on significant methylation sites:

In this study, we have also developed a machine learning model based on all 30791 significant methylation sites to classify between the CRC and control groups. As depicted in Supplementary Table 4, we have achieved balanced parameters using an SVC classifier with the highest AUROC of 0.71 over the training and validation datasets, respectively, with an MCC score of 0.46 over validation.

4.2.3. Feature selection based on Univariate analysis:

To develop a robust prediction method, we have selected the top 25, 15, and 5 positive and negatively correlated methylated sites based on the univariate analysis score. The selected list of top 25, 15 and 5 positive and negative correlated methylated sites can be referred to in Supplementary Table 5.1. Using this approach, we reported the highest AUROC score as 0.88

using a Logistic Regression-based classifier over the top 15 positively correlated methylation sites. Whereas evident from Table 3, we reported the highest AUROC as 0.74 using an Extra tree-based classifier developed using the top 25 negatively correlated methylation sites. The complete results over the training and validation datasets can be referred in Supplementary Table 5.2.

Table 3: Performance of ML-based models over validation dataset developed using top 25, 15 and 5 positive and negative correlated methylation sites based on univariate score.

Top Positively correlated methylated sites							
Name	Features	Thresh	Sens	Spec	Acc	AUROC	MCC
LR	25	0.42	83.87	79.17	81.82	0.87	0.63
LR	15	0.42	83.87	79.17	81.82	0.88	0.63
KN	5	0.60	67.74	79.17	72.73	0.80	0.47
Top Negatively correlated methylated sites							
Name	Features	Thresh	Sens	Spec	Acc	AUROC	MCC
ET	25	0.50	83.87	54.17	70.91	0.74	0.40
RF	15	0.48	80.65	58.33	70.91	0.69	0.40
ET	5	0.52	67.74	58.33	63.64	0.64	0.26

Thresh, Threshold; Sens, Sensitivity; Spec, Specificity; Acc, Accuracy; AUROC, Area Under Receiver Operating Characteristics; MCC, Matthews Correlation Coefficient; LR, Logistic Regression; KN, K-Nearest Neighbor; ET, Extra Trees Classifier; RF, Random Forest

4.2.4. Model developed on selected features by feature selection methods

In addition to this, we have implemented several well-known feature selection algorithms such as Recursive feature selection, Sequential feature selection, and SVC-L1 over the top 100 positively and negatively correlated methylation sites. Again, the top 25, 15, 10 and 5 best features identified as the feature selection results were deployed to train machine learning models. In Table 4, we have reported the best-performing model over the validation dataset using RFE, SFS, and SVC-L1-based feature selection techniques. As evident from Table 4, we observed the MLP-based model outperformed all and reported the highest AUROC as 0.89 and MCC as 0.78 with 25 methylated sites selected using the RFE feature selection technique. In contrast, SVC SVC-based ML model developed using 4 methylated sites extracted using the SFS selection algorithm reported the highest AUROC as 0.76 and MCC score as 0.53.

Table 4: Performance of ML-based models over validation dataset developed using positive and negative correlated methylation sites selected based on feature selection techniques like RFE, SFS, and SVC-L1.

Top Positively correlated methylated sites								
Feature selection	Name	Features	Sens	Spec	Acc	AURO C	MCC	Kappa
RFE	MLP	25	93.10	84.62	89.09	0.89	0.78	0.78
SFS	ET	10	89.66	76.92	83.64	0.83	0.67	0.67
SVC-L1	SVC	9	93.10	65.38	80.00	0.79	0.61	0.59
Top Negatively correlated methylated sites								
Feature selection	Name	Features	Sens	Spec	Acc	AURO C	MCC	Kappa
RFE	NB	25	48.28	96.15	70.91	0.72	0.50	0.43
SFS	SVC	4	75.86	76.92	76.36	0.76	0.53	0.53
SVC-L1	NB	50	55.17	92.31	72.73	0.74	0.51	0.46

#Sens, Sensitivity; Spec, Specificity; Acc, Accuracy; AUROC, Area Under the Curve; MCC, Matthews Correlation Coefficient; SVC, Support Vector Classifier; MLP, Multi-Layer Perceptron; NB, Naïve Bayes;

The list of selected positive and negative correlated methylated sites and their ML model performance score for RFE, SFS and SCV-L1 feature selection techniques can be referred to in Supplementary Tables 6, 7, and 8, respectively.

4.2.5. Deep learning model performance:

In the present study, we have also deployed a deep learning (DL) based model using CNN to investigate the discriminative ability between CRC and normal samples. The performance parameters of the CNN-based model among both groups are depicted in Table 5 for the training and validation sets. As shown, we observed the highest AUROC score of 0.87 and 0.78 on the training and validation datasets, respectively.

Table 5: Performance of DL-based model (CNN) of training and validation sets on 30,479 methylation sites.

Model	Pos	Neg	Spec	Sens	AUROC	Acc	Kappa	MCC
Train	116	103	89.32	84.48	0.87	86.76	0.735	0.737
Validation	26	29	79.31	76.92	0.78	78.18	0.562	0.562

#Pos, Positive; Neg, Negative; Sens, Sensitivity; Spec, Specificity; Acc, Accuracy; AUROC, Area Under the Curve; MCC, Matthews Correlation Coefficient

4.2.6 Functional annotation and gene ontology analysis

The methylation sites for our best-performing model derived from RFE selection were associated with ten protein-coding genes and three intronic regions. The protein-coding genes included T-cell leukemia homeobox (TLX2), Ellis van syndrome gene (EVC), SLIT homolog 3 (SLIT3), Sidekick cell adhesion molecule (SDK1), Brain-specific angiogenesis inhibitor 1 (BAI1), Growth Differentiation Factor 6 (GDF6), Tight Junction Protein 2 (TJP2), complement component 1,q subcomponent like protein (C1QL1), Fibroblast growth factor 4 (FGF4), and hydroxysteroid (17-beta) dehydrogenase 12 (HSD17B12). The function of all these genes is depicted in Table 6. Further, when performing gene enrichment analysis for these genes, we could not identify any tumor-specific pathways and biological/molecular processes associated with our gene set. We identified three molecular functions, including heparin-binding, glycosaminoglycan binding, and sulfur compound binding, as well as two biological processes, including neuron differentiation and generation of neurons.

Table 6: The functional annotation of methylation sites linked with the best-performing model.

S.No.	Chromosome	Start	End	Strand	Gene	Function	References
1	chr2	747426 49	74742 650	-	T-cell Leukemia homeobox (TLX2)	<ul style="list-style-type: none"> ❖ The homeobox-containing (HOX11 family) transcription factor family is majorly involved in cell differentiation and ALK1 signalling. ❖ Crucial for the development of the enteric nervous system. ❖ Loss-of-function of TLX2 is often linked with the tumorigenesis of gastrointestinal stromal tumors. ❖ Involved in the dilatation of the colon. 	TLX2 Gene - GeneCards TLX2 Protein TLX2 Antibody [35]
2	chr4	147559 358	14755 9359	-	Intronic	Not Applicable	-

3	chr4	571330 5	57133 06	+	Ellis van Creveld Syndrome (EVS)	<ul style="list-style-type: none"> ❖ A leucine zipper and transmembrane containing protein that positively regulates ciliary Hedgehog (Hh) signalling. ❖ Crucially involved in endochondral growth as well as skeletal development. 	EVC Gene - GeneCards EVC Protein EVC Antibody [36]
4	chr4	571322 7	57132 28	-	Ellis van Creveld Syndrome (EVS)		
5	chr5	168727 827	16872 7828	+	SLIT homolog 3 (SLIT3)	<ul style="list-style-type: none"> ❖ Molecular guidance cues through cell migration by interacting with roundabout homolog receptors. ❖ Crucial part of SLIT-ROBO signalling and Netrin-signalling. ❖ Involved in soft palate malignancy, breast benign neoplasms, as well as mitochondrial complex deficiency. ❖ It has been suggested to influence thermogenesis and sympathetic activity. ❖ Shown to be inactivated in colorectal cancer. 	SLIT3 Gene - GeneCards SLIT3 Protein SLIT3 Antibody [37–39]
6	chr7	334155 9	33415 60	+	Sidekick cell adhesion molecule (SDK1)	<ul style="list-style-type: none"> ❖ Single-pass transmembrane proteins have extracellular regions composed of an immunoglobulin domain, a fibronectin type III domain, and a short intracellular postsynaptic motif. ❖ Involved in cell junction organization and influences lamina-specific synaptic connections in the retina. ❖ Majorly involved in hypoparathyroidism. ❖ SDK1 mutations have been reported in malignant mesothelioma, adrenocortical carcinoma, lung cancer, as well as in gastric cancer. 	SDK1 Gene - GeneCards SDK1 Protein SDK1 Antibody [40,41]
7	chr7	334156 1	33415 62	+	Sidekick cell adhesion molecule (SDK1)		
8	chr8	143533 657	14353 3658	+	Brain-specific angiogenesis inhibitor 1 (BAI1) (ADGRB1)	<ul style="list-style-type: none"> ❖ BAI1, a member of adhesion G protein-coupled receptors, mediates cell-cell and cell-matrix interactions. ❖ Loss may lead to deficits in neural development. ❖ Responsible for maintaining a balance between initiating and inhibiting new blood vessel formation. 	ADGRB1 Gene - GeneCards AGRBI Protein AGRBI Antibody [42–44]

						<ul style="list-style-type: none"> ❖ Suggested to be transcriptionally regulated by p53 to inhibit angiogenesis in glioblastoma. ❖ Key regulator in immune system processes, phagocytosis, besides cell adhesion. ❖ Crucial in gastric and medulloblastoma oncogenesis due to its role as an angiogenesis inhibitor. ❖ Reduced expression in colorectal cancer. 	
9	chr8	971719 25	97171 926	-	Growth differentiation factor (GDF6)	<ul style="list-style-type: none"> ❖ Responsible for encoding a key ligand for TGF-beta superfamily proteins to recruit and activate SMAD family transcription factors. ❖ Controls proliferation and cellular differentiation in retina/bone formation. ❖ Participates in various signalling pathways like GPCR, ERK signalling, and CREB, besides the GSK3 signalling pathway. ❖ Regulates apoptosis. ❖ Reduced expression of GDF6 in colorectal cancer tissues has been noted. 	GDF6 Gene - GeneCards GDF6 Protein GDF6 Antibody [45–47]
10	chr9	717893 98	71789 399	+	Tight junction protein 2 (TJP2)	<ul style="list-style-type: none"> ❖ Membrane-associated guanylate kinase homologs. ❖ Responsible for membrane-associated guanylate kinase activity and functions as a component of the tight junction and adherens junction barrier in epithelial and endothelial cells. ❖ Transcriptional repression of c-myc, programmed cell death, blood-brain-barrier and immune cell transmigration. 	TJP2 Gene - GeneCards ZO2 Protein ZO2 Antibody [48]
11	chr10	110226 202	11022 6203	-	Intronic	Not Applicable	-
12	chr10	234622 79	23462 280	-	Intronic		

13	chr11	436028 56	43602 857	+	Hydroxysteroid (17-beta) dehydrogenase 12 (HSD17B12)	<ul style="list-style-type: none"> ❖ Mostly expressed in ovarian tissues and is responsible for converting estrone to estradiol. ❖ Involved in fatty acid biosynthesis and metabolism, especially fatty acid elongation. ❖ Responsible for oxidoreductase activity and collagen binding. ❖ Increased risk of death and progression of CRC. 	HSD17B12 Gene - GeneCards DHB12 Protein DHB12 Antibody [49–51]
14	chr11	695891 93	69589 194	-	Fibroblast growth factor 4 (FGF4)	<ul style="list-style-type: none"> ❖ Responsible for mitogenic as well as cell survival activities, including embryonic development, cell growth, morphogenesis, tissue repair, tumor growth and invasion. ❖ Essential in breast cancer-related pathways, MAPK signalling, focal adhesion through PI3K-Akt-mTOR signalling, etc. ❖ Associated with cardiac valve leaflet formation and limb development ❖ Dysregulated in haematological cancers, glioma susceptibility, embryonal carcinoma, etc. 	FGF4 Gene - GeneCards FGF4 Protein FGF4 Antibody [52,53]
15	chr17	430453 19	43045 320	+	Complement component 1, q subcomponent-like 1 (C1QL1)	<ul style="list-style-type: none"> ❖ C1Q complement family characterized by a C-terminal globular gC1Q signature domain involved in the formation of hetero- or homo-trimer. ❖ Signaling receptor binding activity. ❖ Interacts with BAI3 and controls the formation and maintenance of synapses. ❖ Overexpression of C1QL1 has been noted in CRC 	C1QL1 Gene - GeneCards C1QRF Protein C1QRF Antibody [54,55]

The literature and previous evidence show that hypermethylation of CpG islands can silence genes, i.e., suppress the expression of specific genes. The selected methylation sites based on positive correlation (high methylation value in cancerous samples and low methylation value in normal samples) suggested hypermethylation of these CpG regions. To correlate whether hypermethylation of our signature CpG methylation sites is associated with dysregulation of this

gene expression, we explored gene expression patterns of the signature genes in the GEPIA2 server (<http://gepia2.cancer-pku.cn/#index>), which is trained on gene expression patterns of patients submitted on the TCGA database. Table 7 highlighted differentially expressed genes specific for Colon Adenocarcinoma (COAD) and Rectum Adenocarcinoma (READ). Out of 10, 7 (EVC, SLIT3, SDK1, ADGRB1, TJP2, HSD17B12, and C1QL1) genes were significantly expressed in colon and rectum adenocarcinoma. From these seven genes, 5 (EVC, SLIT3, SDK1, ADGRB1, and C1QL1) were predicted to be downregulated, suggesting that increased methylation of these genes in cancer samples could have caused their reduced expression. Two genes (HSD17B12 and TJP2) were overexpressed in both colon and rectum cancers, suggesting that they might have been hypomethylated, paving the way for transcriptional activity. However, more information is required to clearly deduce the correlation between methylation patterns and gene expression of these CpG sites.

Table 7: CpG Signature Genes with differential gene expression from the GEPIA2 database.

S. No.	Gene	Colon Cancer (COAD)		Rectum Cancer (READ)	
		Significance ($p_{adj} < 0.05$)	Regulation ($\log_2\text{FoldChange}$)	Significance ($p_{adj} < 0.05$)	Regulation ($\log_2\text{FoldChange}$)
1	T-cell Leukemia homeobox (TLX2)	-	-	-	-
2	Ellis van Creveld Syndrome (EVC)	Yes, 2.55e-33	Downregulated (-1.619)	Yes, 1.98e-15	Downregulated (-1.752)
3	SLIT homolog 3 (SLIT3)	Yes, 9.59e-51	Downregulated (-2.358)	Yes, 2.09e-22	Downregulated (-2.305)
4	Sidekick cell adhesion molecule (SDK1)	Yes, 1.65e-39	Downregulated (-1.638)	Yes, 1.18e-20	Downregulated (-1.733)
5	Brain-specific angiogenesis inhibitor 1 (BAI1) / ADGRB1	Yes, 9.03e-67	Downregulated (-1.006)	Yes, 4.64e-38	Downregulated (-1.116)
6	Growth differentiation factor (GDF6)	-	-	-	-
7	Tight junction protein 2 (TJP2)	Yes, 3.52e-48	Upregulated (1.229)	Yes, 1.45e-25	Upregulated (1.364)
8	Hydroxysteroid (17-beta) dehydrogenase 12 (HSD17B12)	Yes, 4.12e-71	Upregulated (1.422)	Yes, 1.40e-33	Upregulated (1.508)
9	Fibroblast growth factor 4 (FGF4)	-	-	-	-

10	Complement component 1, q subcomponent-like 1 (C1QL1)	Yes, 3.91e-70	Downregulated (-1.456)	Yes, 4.61e-30	Downregulated (-1.480)
----	---	------------------	---------------------------	------------------	---------------------------

3.5. Conclusion

Colorectal cancer is a multifactorial disorder whose incidence and mortality are increasing daily due to a lack of panels for detecting CRC early in individuals. In conclusion, our study demonstrates the effectiveness of a univariate correlation statistics-based approach in identifying high-priority methylation sites for early colorectal cancer detection. We identified a panel of 15 upregulated methylation sites on EVC, FRMD6, FRMD6-AS2, LHFPL6, LIFR, and ZFPM2, along with three intergenic regions, as optimal classifiers. Using a random forest (RF)-based machine learning model, our approach achieved a specificity of 86.21% and sensitivity of 88.46%, comparable to the widely used methylated SEPTIN9 assay (88% specificity, 90% sensitivity). These findings underscore the potential of cfDNA methylation markers in enhancing non-invasive CRC detection and warrant further validation in clinical settings.

Funding Source

The current work has been supported by the Department of Biotechnology (DBT) grant BT/PR40158/BTIS/137/24/2021.

Conflict of interest

The authors declare no competing financial and non-financial interests.

Authors' contributions

KM collected the dataset. KM, SJ, and NK processed the dataset. KM, NK, and GPSR implemented the algorithms and developed the prediction models. NK, SJ, KM, and GPSR analysed the results. NB, SJ, KM, NK, and GPSR performed the writing, reviewing, and draft preparation of the manuscript. GPSR conceived and coordinated the project. All authors have read and approved the final manuscript.

Acknowledgments

Authors are thankful to the University Grants Commission (UGC), Council of Scientific & Industrial Research (CSIR), and IIT-Delhi for fellowships and financial support, and the Department of Computational Biology, IIITD New Delhi, for infrastructure and facilities.

References

- [1] Baojun Duan ^{1 2} , Yaning Zhao ¹ , Jun Bai ² , Jianhua Wang ³ , Xianglong Duan ^{3 4} , Xiaohui Luo ¹ , Rong Zhang ⁵ , Yansong Pu ³ , Mingqing Kou ⁶ , Jianyuan Lei ⁷ , Shangzhen Yang ⁸ Jose Andres Morgado-Diaz ¹ , editors., Colorectal Cancer: An Overview, Gastrointestinal Cancers [Internet]., Brisbane (AU): Exon Publications, 2022. <https://doi.org/10.36255/exon-publications-gastrointestinal-cancers-colorectal-cancer>.
- [2] H. Song, C. Ruan, Y. Xu, T. Xu, R. Fan, T. Jiang, M. Cao, J. Song, Survival stratification for colorectal cancer via multi-omics integration using an autoencoder-based model, *Exp. Biol. Med. (Maywood)* 247 (2022) 898–909. <https://doi.org/10.1177/15353702211065010>.
- [3] S.T. Krishnan, D. Winkler, D. Creek, D. Anderson, C. Kirana, G.J. Maddern, K. Fenix, E. Hauben, D. Rudd, N.H. Voelcker, Staging of colorectal cancer using lipid biomarkers and machine learning, *Metabolomics* 19 (2023) 84. <https://doi.org/10.1007/s11306-023-02049-z>.
- [4] R.L. Siegel, A.N. Giaquinto, A. Jemal, Cancer statistics, 2024, *CA Cancer J. Clin.* 74 (2024) 12–49. <https://doi.org/10.3322/caac.21820>.
- [5] E.P. Whitlock, J. Lin, E. Liles, T. Beil, R. Fu, E. O'Connor, R.N. Thompson, T. Cardenas, Screening for colorectal cancer: An updated systematic review, Agency for Healthcare Research and Quality (US), Rockville (MD), 2008. <https://www.ncbi.nlm.nih.gov/pubmed/20722162>.
- [6] W. Atkin, Options for screening for colorectal cancer, *Scand. J. Gastroenterol. Suppl.* (2003) 13–16. <https://doi.org/10.1080/00855910310001421>.
- [7] R.S. Bresalier, C. Senore, G.P. Young, J. Allison, R. Benamouzig, S. Benton, P.M.M. Bossuyt, L. Caro, B. Carvalho, H.-M. Chiu, V.M.H. Coupé, W. de Klaver, C.M. de Klerk, E. Dekker, S. Dolwani, C.G. Fraser, W. Grady, L. Guittet, S. Gupta, S.P. Halloran, U. Haug, G. Hoff, S. Itzkowitz, T. Kortlever, A. Koulaouzidis, U. Ladabaum, B. Lauby-Secretan, M. Leja, B. Levin, T.R. Levin, F. Macrae, G.A. Meijer, J. Melson, C. O'Morain, S. Parry, L. Rabeneck, D.F. Ransohoff, R. Sáenz, H. Saito, S. Sanduleanu-Dascalescu, R.E. Schoen, K.

- Selby, H. Singh, R.J.C. Steele, J.J.Y. Sung, E.L. Symonds, S.J. Winawer, Members of the World Endoscopy Colorectal Cancer Screening New Test Evaluation Expert Working Group, An efficient strategy for evaluating new non-invasive screening tests for colorectal cancer: the guiding principles, *Gut* 72 (2023) 1904–1918. <https://doi.org/10.1136/gutjnl-2023-329701>.
- [8] K. Garborg, Ø. Holme, M. Løberg, M. Kalager, H.O. Adami, M. Bretthauer, Current status of screening for colorectal cancer, *Ann. Oncol.* 24 (2013) 1963–1972. <https://doi.org/10.1093/annonc/mdt157>.
- [9] C. Senore, C. Doubeni, L. Guittet, FIT as a comparator for evaluating the effectiveness of new non-invasive CRC screening test, *Dig. Dis. Sci.* (2024). <https://doi.org/10.1007/s10620-024-08718-w>.
- [10] R. Gómez-Molina, M. Suárez, R. Martínez, M. Chilet, J.M. Bauça, J. Mateo, Utility of stool-based tests for colorectal cancer detection: A comprehensive review, *Healthcare (Basel)* 12 (2024) 1645. <https://doi.org/10.3390/healthcare12161645>.
- [11] S. Grego, C.M. Welling, G.H. Miller, P.F. Coggan, K.L. Sellgren, B.T. Hawkins, G.S. Ginsburg, J.R. Ruiz, D.A. Fisher, B.R. Stoner, A hands-free stool sampling system for monitoring intestinal health and disease, *Sci. Rep.* 12 (2022) 10859. <https://doi.org/10.1038/s41598-022-14803-9>.
- [12] A.Z. Gimeno-García, E. Quintero, Role of colonoscopy in colorectal cancer screening: Available evidence, *Best Pract. Res. Clin. Gastroenterol.* 66 (2023) 101838. <https://doi.org/10.1016/j.bpg.2023.101838>.
- [13] P.S. Liang, J.A. Dominitz, Colorectal cancer screening: Is colonoscopy the best option?, *Med. Clin. North Am.* 103 (2019) 111–123. <https://doi.org/10.1016/j.mena.2018.08.010>.
- [14] M.D. Knudsen, K. Wang, L. Wang, G. Polychronidis, P. Berstad, A. Hjartåker, Z. Fang, S. Ogino, A.T. Chan, M. Song, Colorectal cancer incidence and mortality after negative colonoscopy screening results, *JAMA Oncol.* 11 (2025) 46–54. <https://doi.org/10.1001/jamaoncol.2024.5227>.
- [15] C.M. Spiceland, N. Lodhia, Endoscopy in inflammatory bowel disease: Role in diagnosis, management, and treatment, *World J. Gastroenterol.* 24 (2018) 4014–4020. <https://doi.org/10.3748/wjg.v24.i35.4014>.

- [16] P.W.W. Chan, J.H. Ngu, Z. Poh, R. Soetikno, Colorectal cancer screening, *Singapore Med. J.* 58 (2017) 24–28. <https://doi.org/10.11622/smedj.2017004>.
- [17] S.W. Chung, S. Hakim, S. Siddiqui, B.D. Cash, Update on flexible sigmoidoscopy, computed tomographic colonography, and capsule colonoscopy, *Gastrointest. Endosc. Clin. N. Am.* 30 (2020) 569–583. <https://doi.org/10.1016/j.giec.2020.02.009>.
- [18] Q.-N. Liu, Y. Ye, X.-Q. Jia, Role of different examination methods in colorectal cancer screening: Insights and future directions, *World J. Gastroenterol.* 30 (2024) 4741–4744. <https://doi.org/10.3748/wjg.v30.i44.4741>.
- [19] E. Halilovic, I. Rasic, A. Sofic, A. Mujic, A. Rovcanin, E. Hodzic, E. Kulovic, The importance of determining preoperative serum concentration of Carbohydrate antigen 19-9 and Carcinoembryonic antigen in assessing the progression of colorectal cancer, *Med. Arch.* 74 (2020) 346–349. <https://doi.org/10.5455/medarh.2020.74.346-349>.
- [20] R.A. Rittgers, G. Steele Jr, N. Zamcheck, M.S. Loewenstein, P.H. Sugarbaker, R.J. Mayer, J.J. Lokich, J. Maltz, R.E. Wilso, Transient carcinoembryonic antigen (CEA) elevations following resection of colorectal cancer: a limitation in the use of serial CEA levels as an indicator for second-look surgery, *J. Natl. Cancer Inst.* 61 (1978) 315–318. <https://www.ncbi.nlm.nih.gov/pubmed/277718>.
- [21] X. Li, L. Stassen, P. Schrotz-King, Z. Zhao, R. Cardoso, J.R. Raut, M. Bhardwaj, H. Brenner, Potential of fecal carcinoembryonic antigen for noninvasive detection of colorectal cancer: A systematic review, *Cancers (Basel)* 15 (2023) 5656. <https://doi.org/10.3390/cancers15235656>.
- [22] M.G. Fakh, A. Padmanabhan, CEA monitoring in colorectal cancer. What you should know, *Oncology (Williston Park)* 20 (2006) 579–87; discussion 588, 594, 596 passim. <https://www.ncbi.nlm.nih.gov/pubmed/16773844>.
- [23] J. Stikma, D.C. Grootendorst, P.W.G. van der Linden, CA 19-9 as a marker in addition to CEA to monitor colorectal cancer, *Clin. Colorectal Cancer* 13 (2014) 239–244. <https://doi.org/10.1016/j.clcc.2014.09.004>.
- [24] L. Lakemeyer, S. Sander, M. Wittau, D. Henne-Bruns, M. Kornmann, J. Lemke, Diagnostic and prognostic value of CEA and CA19-9 in colorectal cancer, *Diseases* 9 (2021) 21. <https://doi.org/10.3390/diseases9010021>.

- [25] J. Hu, B. Hu, Y.-C. Gui, Z.-B. Tan, J.-W. Xu, Diagnostic value and clinical significance of methylated SEPT9 for colorectal cancer: A meta-analysis, *Med. Sci. Monit.* 25 (2019) 5813–5822. <https://doi.org/10.12659/MSM.915472>.
- [26] J.D. Warren, W. Xiong, A.M. Bunker, C.P. Vaughn, L.V. Furtado, W.L. Roberts, J.C. Fang, W.S. Samowitz, K.A. Heichman, Septin 9 methylated DNA is a sensitive and specific blood test for colorectal cancer, *BMC Med.* 9 (2011) 133. <https://doi.org/10.1186/1741-7015-9-133>.
- [27] K. Ashouri, A. Wong, P. Mittal, L. Torres-Gonzalez, J.H. Lo, S. Soni, S. Algaze, T. Khoukaz, W. Zhang, Y. Yang, J. Millstein, H.-J. Lenz, F. Battaglin, Exploring predictive and prognostic biomarkers in colorectal cancer: A comprehensive review, *Cancers (Basel)* 16 (2024) 2796. <https://doi.org/10.3390/cancers16162796>.
- [28] L. Dong, H. Ren, Blood-based DNA methylation biomarkers for early detection of colorectal cancer, *J. Proteomics Bioinform.* 11 (2018) 120–126. <https://doi.org/10.4172/jpb.1000477>.
- [29] A.G. Vaiopoulos, K.C. Athanasoula, A.G. Papavassiliou, Epigenetic modifications in colorectal cancer: molecular insights and therapeutic challenges, *Biochim. Biophys. Acta* 1842 (2014) 971–980. <https://doi.org/10.1016/j.bbadis.2014.02.006>.
- [30] H.Y.S. Essa, G. Kusaf, O. Yuruker, R. Kalkan, Epigenetic alteration in colorectal cancer: A biomarker for diagnostic and therapeutic application, *Glob. Med. Genet.* 9 (2022) 258–262. <https://doi.org/10.1055/s-0042-1757404>.
- [31] Y. Li, J. Xiao, T. Zhang, Y. Zheng, H. Jin, Analysis of KRAS, NRAS, and BRAF mutations, microsatellite instability, and relevant prognosis effects in patients with early colorectal cancer: A cohort study in east Asia, *Front. Oncol.* 12 (2022) 897548. <https://doi.org/10.3389/fonc.2022.897548>.
- [32] J. Taieb, F.A. Sinicrope, L. Pederson, S. Lonardi, S.R. Alberts, T.J. George, G. Yothers, E. Van Cutsem, L. Saltz, S. Ogino, R. Kerr, T. Yoshino, R.M. Goldberg, T. André, P. Laurent-Puig, Q. Shi, Different prognostic values of KRAS exon 2 submutations and BRAF V600E mutation in microsatellite stable (MSS) and unstable (MSI) stage III colon cancer: an ACCENT/IDEA pooled analysis of seven trials, *Ann. Oncol.* 34 (2023) 1025–1034. <https://doi.org/10.1016/j.annonc.2023.08.006>.

- [33] J. González-Montero, C.I. Rojas, M. Burotto, Predictors of response to immunotherapy in colorectal cancer, *Oncologist* 29 (2024) 824–832. <https://doi.org/10.1093/oncolo/oyae152>.
- [34] Z. Tang, B. Kang, C. Li, T. Chen, Z. Zhang, GEPIA2: an enhanced web server for large-scale expression profiling and interactive analysis, *Nucleic Acids Res.* 47 (2019) W556–W560. <https://doi.org/10.1093/nar/gkz430>.
- [35] B. Chen, X. Ding, A. Wan, X. Qi, X. Lin, H. Wang, W. Mu, G. Wang, J. Zheng, Author Correction: Comprehensive analysis of TLX2 in pan cancer as a prognostic and immunologic biomarker and validation in ovarian cancer, *Sci. Rep.* 13 (2023) 17678. <https://doi.org/10.1038/s41598-023-44831-y>.
- [36] A. Kowal, A. Mostowska, D. Mydlak, B. Eberdt-Goląbek, M. Misztal, P.P. Jagodziński, K.K. Hozyasz, EVC gene polymorphisms and risks of isolated hypospadias - a preliminary study, *Cent. European J. Urol.* 68 (2015) 257–262. <https://doi.org/10.5173/ceju.2015.493>.
- [37] H.J. Cho, H. Kim, Y.-S. Lee, S.A. Moon, J.-M. Kim, H. Kim, M.J. Kim, J. Yu, K. Kim, I.-J. Baek, S.H. Lee, K.H. Ahn, S. Kim, J.-S. Kang, J.-M. Koh, SLIT3 promotes myogenic differentiation as a novel therapeutic factor against muscle loss, *J. Cachexia Sarcopenia Muscle* 12 (2021) 1724–1740. <https://doi.org/10.1002/jcsm.12769>.
- [38] L. Ng, A.K.M. Chow, J.H.W. Man, T.C.C. Yau, T.M.H. Wan, D.N. Iyer, V.H.T. Kwan, R.T.P. Poon, R.W.C. Pang, W.-L. Law, Suppression of Slit3 induces tumor proliferation and chemoresistance in hepatocellular carcinoma through activation of GSK3 β / β -catenin pathway, *BMC Cancer* 18 (2018) 621. <https://doi.org/10.1186/s12885-018-4326-5>.
- [39] Y.-N. Wang, Y. Tang, Z. He, H. Ma, L. Wang, Y. Liu, Q. Yang, D. Pan, C. Zhu, S. Qian, Q.-Q. Tang, Slit3 secreted from M2-like macrophages increases sympathetic activity and thermogenesis in adipose tissue, *Nat. Metab.* 3 (2021) 1536–1551. <https://doi.org/10.1038/s42255-021-00482-9>.
- [40] M. Yamagata, Structure and functions of sidekicks, *Front. Mol. Neurosci.* 13 (2020) 139. <https://doi.org/10.3389/fnmol.2020.00139>.
- [41] K.M. Goodman, M. Yamagata, X. Jin, S. Mannepalli, P.S. Katsamba, G. Ahlsén, A.P. Sergeeva, B. Honig, J.R. Sanes, L. Shapiro, Molecular basis of sidekick-mediated cell-cell adhesion and specificity, *Elife* 5 (2016). <https://doi.org/10.7554/eLife.19058>.
- [42] R.R. Parag, T. Yamamoto, K. Saito, D. Zhu, L. Yang, E.G. Van Meir, Novel isoforms of adhesion G protein-coupled receptor B1 (ADGRB1/BAI1) generated from an alternative

- promoter in intron 17, *Mol. Neurobiol.* 62 (2025) 900–917. <https://doi.org/10.1007/s12035-024-04293-3>.
- [43] G. Aust, D. Zhu, E.G. Van Meir, L. Xu, Adhesion GPCRs in tumorigenesis, *Handb. Exp. Pharmacol.* 234 (2016) 369–396. https://doi.org/10.1007/978-3-319-41523-9_17.
- [44] Y. Fukushima, Y. Oshika, T. Tsuchida, T. Tokunaga, H. Hatanaka, H. Kijima, H. Yamazaki, Y. Ueyama, N. Tamaoki, M. Nakamura, Brain-specific angiogenesis inhibitor 1 expression is inversely correlated with vascularity and distant metastasis of colorectal cancer, *Int. J. Oncol.* 13 (1998) 967–970. <https://doi.org/10.3892/ijo.13.5.967>.
- [45] A.J. Pellatt, L.E. Mullany, J.S. Herrick, L.C. Sakoda, R.K. Wolff, W.S. Samowitz, M.L. Slattery, The TGF β -signaling pathway and colorectal cancer: associations between dysregulated genes and miRNAs, *J. Transl. Med.* 16 (2018) 191. <https://doi.org/10.1186/s12967-018-1566-8>.
- [46] S. Krispin, A.N. Stratman, C.H. Melick, R.V. Stan, M. Malinverno, J. Gleklen, D. Castranova, E. Dejana, B.M. Weinstein, Growth differentiation factor 6 promotes vascular stability by restraining vascular endothelial growth factor signaling, *Arterioscler. Thromb. Vasc. Biol.* 38 (2018) 353–362. <https://doi.org/10.1161/ATVBAHA.117.309571>.
- [47] H. Cui, J. Zhang, Z. Li, F. Chen, H. Cui, X. Du, H. Liu, J. Wang, A.D. Diwan, Z. Zheng, Growth differentiation factor-6 attenuates inflammatory and pain-related factors and degenerated disc-induced pain behaviors in rat model, *J. Orthop. Res.* 39 (2021) 959–970. <https://doi.org/10.1002/jor.24793>.
- [48] J. Tang, M. Tan, Y. Deng, H. Tang, H. Shi, M. Li, W. Ma, J. Li, H. Dai, J. Li, S. Zhou, X. Li, F. Wei, X. Ma, L. Luo, Two novel pathogenic variants of TJP2 gene and the underlying molecular mechanisms in progressive familial intrahepatic cholestasis type 4 patients, *Front. Cell Dev. Biol.* 9 (2021) 661599. <https://doi.org/10.3389/fcell.2021.661599>.
- [49] H. Heikelä, S.T. Ruohonen, M. Adam, R. Viitanen, H. Liljenbäck, O. Eskola, M. Gabriel, L. Mairinoja, A. Pessia, V. Velagapudi, A. Roivainen, F.-P. Zhang, L. Strauss, M. Poutanen, Hydroxysteroid (17 β) dehydrogenase 12 is essential for metabolic homeostasis in adult mice, *Am. J. Physiol. Endocrinol. Metab.* 319 (2020) E494–E508. <https://doi.org/10.1152/ajpendo.00042.2020>.
- [50] H. Kemiläinen, M. Adam, J. Mäki-Jouppila, P. Damdimopoulou, A.E. Damdimopoulos, J. Kere, O. Hovatta, T.D. Laajala, T. Aittokallio, J. Adamski, H. Ryberg, C. Ohlsson, L.

- Strauss, M. Poutanen, The hydroxysteroid (17 β) dehydrogenase family gene HSD17B12 is involved in the prostaglandin synthesis pathway, the ovarian function, and regulation of fertility, *Endocrinology* 157 (2016) 3719–3730. <https://doi.org/10.1210/en.2016-1252>.
- [51] Y. Lin, Y. Meng, J. Zhang, L. Ma, L. Jiang, Y. Zhang, M. Yuan, A. Ren, W. Zhu, S. Li, Y. Shu, M. Du, L. Zhu, Functional genetic variant of HSD17B12 in the fatty acid biosynthesis pathway predicts the outcome of colorectal cancer, *J. Cell. Mol. Med.* 24 (2020) 14160–14170. <https://doi.org/10.1111/jcmm.16026>.
- [52] A. Beenken, M. Mohammadi, The FGF family: biology, pathophysiology and therapy, *Nat. Rev. Drug Discov.* 8 (2009) 235–253. <https://doi.org/10.1038/nrd2792>.
- [53] C.-S. Li, S.-X. Zhang, H.-J. Liu, Y.-L. Shi, L.-P. Li, X.-B. Guo, Z.-H. Zhang, Fibroblast growth factor receptor 4 as a potential prognostic and therapeutic marker in colorectal cancer, *Biomarkers* 19 (2014) 81–85. <https://doi.org/10.3109/1354750X.2013.876555>.
- [54] S. Moghimyfiroozabad, M.A. Paul, S.M. Sigoillot, F. Selimi, Mapping and targeting of C1ql1-expressing cells in the mouse, *Sci. Rep.* 13 (2023) 17563. <https://doi.org/10.1038/s41598-023-42924-2>.
- [55] X. Qiu, J.-R. Feng, F. Wang, P.-F. Chen, X.-X. Chen, R. Zhou, Y. Chang, J. Liu, Q. Zhao, Profiles of differentially expressed genes and overexpression of NEBL indicates a positive prognosis in patients with colorectal cancer, *Mol. Med. Rep.* 17 (2018) 3028–3034. <https://doi.org/10.3892/mmr.2017.8210>.

SUPPLEMENTARY TABLES

Supplementary Table 1: Unique ID representation of the top 100 positive and negative significantly methylated CpG sites.

Site ID	Chromosome no.	Start	End	Strand	Gene Symbol
181489	chr7	155164740	155164741	-	NA
196741	chr8	73163886	73163887	-	NA
196742	chr8	73163878	73163879	-	NA
181490	chr7	155164736	155164737	-	NA
181491	chr7	155164721	155164722	-	NA
93487	chr1	181287827	181287828	+	NA
38139	chr14	51560392	51560393	-	TRIM9
86829	chr19	58952130	58952131	+	CTD-2619J13.19
189090	chr8	105479178	105479179	+	NA
164637	chr5	38556294	38556295	+	LIFR
197569	chr8	97157394	97157395	-	GDF6
33055	chr13	39262101	39262102	+	FREM2
19308	chr11	69589200	69589201	-	FGF4
155363	chr4	5713260	5713261	+	EVC
93488	chr1	181287836	181287837	+	NA
19307	chr11	69589207	69589208	-	FGF4
155366	chr4	5713272	5713273	+	EVC
164638	chr5	38556301	38556302	+	LIFR
109113	chr20	21377300	21377301	-	NKX2-4

155364	chr4	5713266	5713267	+	EVC
22040	chr12	108237684	108237685	+	NA
140674	chr3	128274241	128274242	+	NA
155365	chr4	5713270	5713271	+	EVC
140673	chr3	128274237	128274238	+	NA
162111	chr5	168727791	168727792	+	NA
14879	chr11	31821271	31821272	-	PAX6
197621	chr8	97171940	97171941	-	GDF6
53523	chr16	55513384	55513385	+	MMP2
22039	chr12	108237667	108237668	+	RP11-554D14.6
19310	chr11	69589193	69589194	-	FGF4
19309	chr11	69589198	69589199	-	FGF4
109111	chr20	21377305	21377306	-	NKX2-4
53525	chr16	55513398	55513399	+	MMP2
32305	chr13	26042782	26042783	+	ATP8A2
140675	chr3	128274243	128274244	+	NA
32433	chr13	27334449	27334450	-	GPR12
14880	chr11	31821265	31821266	-	PAX6
142220	chr3	156009151	156009152	-	NA
53524	chr16	55513389	55513390	+	MMP2
33056	chr13	39262113	39262114	+	FREM2
32303	chr13	26042768	26042769	+	ATP8A2
190943	chr8	143533657	143533658	+	NA
162112	chr5	168727793	168727794	+	SLIT3
40169	chr14	77737465	77737466	+	NGB

190944	chr8	143533662	143533663	+	NA
190942	chr8	143533649	143533650	+	NA
197570	chr8	97157391	97157392	-	GDF6
22768	chr12	113909259	113909260	+	NA
140676	chr3	128274247	128274248	+	NA
155367	chr4	5713287	5713288	+	EVC
162113	chr5	168727797	168727798	+	NA
14654	chr11	2890925	2890926	+	NA
30599	chr13	110960276	110960277	+	NA
32304	chr13	26042777	26042778	+	ATP8A2
140677	chr3	128274252	128274253	+	NA
150767	chr4	147559372	147559373	-	NA
14878	chr11	31821274	31821275	-	PAX6
109107	chr20	21377312	21377313	-	NKX2-4
163975	chr5	1883206	1883207	-	IRX4
140678	chr3	128274261	128274262	+	NA
30600	chr13	110960289	110960290	+	NA
15646	chr11	43602856	43602857	+	HSD17B12
150771	chr4	147559354	147559355	-	NA
150770	chr4	147559358	147559359	-	NA
62691	chr17	43045319	43045320	+	C1QL1
15643	chr11	43602844	43602845	+	HSD17B12
15645	chr11	43602854	43602855	+	HSD17B12
35227	chr14	102030060	102030061	-	NA
155368	chr4	5713291	5713292	+	EVC

206115	chr9	71789398	71789399	+	TJP2
162114	chr5	168727809	168727810	+	NA
30601	chr13	110960292	110960293	+	NA
145032	chr3	32858836	32858837	+	NA
145033	chr3	32858838	32858839	+	NA
197622	chr8	97171925	97171926	-	GDF6
155369	chr4	5713302	5713303	+	EVC
15644	chr11	43602846	43602847	+	HSD17B12
140679	chr3	128274264	128274265	+	NA
150768	chr4	147559368	147559369	-	NA
19311	chr11	69589170	69589171	-	FGF4
137612	chr2	74742649	74742650	-	TLX2
162115	chr5	168727813	168727814	+	NA
14336	chr11	20618762	20618763	+	NA
40170	chr14	77737494	77737495	+	NGB
155370	chr4	5713305	5713306	+	EVC
184473	chr7	3341549	3341550	+	SDK1, AC073316.1
155374	chr4	5713227	5713228	-	EVC
150773	chr4	147559337	147559338	-	NA
1154	chr10	110226219	110226220	-	NA
137625	chr2	74743101	74743102	-	TLX2
162118	chr5	168727827	168727828	+	NA
184474	chr7	3341554	3341555	+	SDK1, AC073316.1
198323	chr9	101706252	101706253	-	NA
198324	chr9	101706249	101706250	-	NA

184476	chr7	3341561	3341562	+	SDK1, AC073316.1
184475	chr7	3341559	3341560	+	SDK1, AC073316.1
40171	chr14	77737503	77737504	+	NGB
1155	chr10	110226204	110226205	-	NA
1156	chr10	110226202	110226203	-	NA
5779	chr10	23462279	23462280	-	NA
3658	chr10	134527979	134527980	+	INPP5A
100955	chr1	2980307	2980308	-	LINC00982
24643	chr12	132837553	132837554	-	GALNT9
24644	chr12	132837550	132837551	-	NA
75322	chr19	1071393	1071394	-	HMHA1
100957	chr1	2980290	2980291	-	LINC00982
75321	chr19	1071397	1071398	-	HMHA1
189313	chr8	1105774	1105775	+	CTD-2281E23.2
100956	chr1	2980300	2980301	-	LINC00982
174999	chr6	42227350	42227351	+	TRERF1
9374	chr10	75492828	75492829	-	GLUD1P3, DUSP8P5
24639	chr12	132837590	132837591	-	GALNT9
180703	chr7	150095096	150095097	-	ZNF775
100954	chr1	2980316	2980317	-	LINC00982
125190	chr2	107459700	107459701	+	NA
54573	chr16	67686958	67686959	-	RLTPR
9375	chr10	75492825	75492826	-	GLUD1P3, DUSP8P5
114431	chr20	62403000	62403001	-	ZBTB46
180704	chr7	150095094	150095095	-	ZNF775

180705	chr7	150095090	150095091	-	NA
75318	chr19	1071414	1071415	-	HMHA1
7577	chr10	48429234	48429235	-	GDF10
116026	chr21	36164307	36164308	-	RUNX1
125191	chr2	107459708	107459709	+	ST6GAL2
75320	chr19	1071405	1071406	-	HMHA1
17992	chr11	65307223	65307224	+	LTBP3
7575	chr10	48429245	48429246	-	GDF10
24642	chr12	132837571	132837572	-	GALNT9
100953	chr1	2980333	2980334	-	LINC00982
75319	chr19	1071410	1071411	-	HMHA1
126874	chr2	129077403	129077404	+	NA
203525	chr9	140173334	140173335	-	TOR4A
24640	chr12	132837583	132837584	-	GALNT9
78188	chr19	17952552	17952553	+	JAK3
24641	chr12	132837574	132837575	-	NA
27300	chr12	52473709	52473710	+	RP11-1100L3.7, OR7E47P
36304	chr14	105609046	105609047	-	JAG2
75616	chr19	1122710	1122711	-	SBNO2
171893	chr6	167315154	167315155	-	RPS6KA2, RP11-514O12.4
126871	chr2	129077345	129077346	+	NA
97256	chr1	228399680	228399681	-	NA
54574	chr16	67686950	67686951	-	RLTPR
36303	chr14	105609051	105609052	-	NA

202311	chr9	138663007	138663008	+	NA
99171	chr1	243637779	243637780	+	SDCCAG8
126873	chr2	129077362	129077363	+	NA
7576	chr10	48429242	48429243	-	GDF10
7701	chr10	49659121	49659122	+	ARHGAP22
7574	chr10	48429250	48429251	-	GDF10
149453	chr4	11401606	11401607	-	HS3ST1
7573	chr10	48429258	48429259	-	GDF10
78187	chr19	17952537	17952538	+	JAK3
99172	chr1	243637788	243637789	+	SDCCAG8
75129	chr19	1046977	1046978	+	ABCA7
126872	chr2	129077352	129077353	+	NA
99173	chr1	243637791	243637792	+	SDCCAG8
90819	chr1	151104697	151104698	+	SEMA6C
74073	chr18	76782750	76782751	-	NA
62822	chr17	43473133	43473134	+	ARHGAP27
7700	chr10	49659115	49659116	+	ARHGAP22
89080	chr1	112525331	112525332	-	KCND3
36305	chr14	105609043	105609044	-	JAG2
160627	chr5	140052645	140052646	+	NA
9376	chr10	75492819	75492820	-	GLUD1P3, DUSP8P5
7699	chr10	49659109	49659110	+	ARHGAP22
123337	chr22	49935076	49935077	+	C22orf34
7703	chr10	49659153	49659154	+	ARHGAP22
57404	chr16	88721882	88721883	+	MVD

35413	chr14	103373909	103373910	-	NA
90817	chr1	151104661	151104662	+	SEMA6C
133220	chr2	241989342	241989343	+	NA
127235	chr2	132415683	132415684	+	NA
18002	chr11	65307164	65307165	-	LTBP3
17680	chr11	64533706	64533707	+	SF1
202310	chr9	138662999	138663000	+	KCNT1
113054	chr20	58514147	58514148	+	FAM217B, PPP1R3D
58323	chr17	10541763	10541764	+	MYH3
75317	chr19	1071419	1071420	-	HMHA1
90224	chr1	1375230	1375231	-	VWA1
78181	chr19	17942591	17942592	+	JAK3
30580	chr13	110918389	110918390	-	NA
116025	chr21	36164318	36164319	-	RUNX1
35412	chr14	103373932	103373933	-	TRAF3
35411	chr14	103373938	103373939	-	TRAF3
35414	chr14	103373907	103373908	-	NA
202309	chr9	138662987	138662988	+	KCNT1
123336	chr22	49935066	49935067	+	C22orf34
24632	chr12	132837654	132837655	+	GALNT9
189312	chr8	1105760	1105761	+	CTD-2281E23.2
24631	chr12	132837641	132837642	+	NA
41489	chr15	101099302	101099303	+	NA
54571	chr16	67686982	67686983	-	RLTPR
24476	chr12	132393497	132393498	+	ULK1

54570	chr16	67686988	67686989	-	RLTPR
84787	chr19	49183853	49183854	-	SEC1P
41491	chr15	101099317	101099318	+	RP11-526I2.1
204581	chr9	34372181	34372182	-	KIAA1161
41490	chr15	101099305	101099306	+	RP11-526I2.1
54572	chr16	67686964	67686965	-	RLTPR
30581	chr13	110918379	110918380	-	COL4A1

Supplementary Table 2: Statistical analysis of the top 100 positive and negative significantly methylated CpG sites

Site ID	Mean_ CRC	StdDev_ CRC	Variance_ CRC	Mean_ NOR	StdDev_ NOR	Variance_ NOR	Abs_Mean _Diff	Univariate score	t-test score	p-value
181489	5.27	9.44	89.05	0.63	1.46	2.13	4.64	0.43	5.59	5.47E-08
196741	6.48	13.55	183.73	0.50	1.33	1.77	5.98	0.40	5.05	0.000000824
196742	6.15	13.11	171.79	0.37	1.03	1.07	5.78	0.41	5.05	0.000000805
181490	4.38	8.49	72.06	0.38	1.17	1.36	4.00	0.41	5.37	0.000000169
181491	3.33	7.24	52.40	0.12	0.52	0.27	3.21	0.41	5.08	0.000000688
93487	3.33	7.17	51.43	0.15	0.52	0.27	3.19	0.41	5.09	0.000000664
38139	7.06	14.88	221.27	0.61	1.32	1.74	6.44	0.40	4.96	0.00000125
86829	3.96	7.02	49.23	0.61	1.32	1.75	3.35	0.40	5.40	0.000000146
189090	3.00	4.57	20.91	0.61	1.32	1.75	2.40	0.41	5.80	1.82E-08
164637	3.00	6.71	45.01	0.12	0.52	0.27	2.87	0.40	4.91	0.00000158
197569	2.47	5.20	27.01	0.13	0.48	0.23	2.34	0.41	5.14	0.000000522
33055	10.08	14.67	215.31	2.46	2.99	8.92	7.62	0.43	5.85	0.000000014
19308	3.39	7.60	57.79	0.09	0.34	0.11	3.30	0.42	4.99	0.0000011

155363	2.85	4.97	24.72	0.34	1.11	1.24	2.50	0.41	5.65	4.05E-08
93488	2.98	6.85	46.96	0.08	0.35	0.12	2.90	0.40	4.86	0.00000203
19307	4.02	8.09	65.38	0.38	0.92	0.85	3.64	0.40	5.14	0.000000515
155366	2.45	4.69	22.01	0.10	0.40	0.16	2.35	0.46	5.74	2.57E-08
164638	2.70	6.05	36.60	0.11	0.44	0.20	2.59	0.40	4.91	0.00000158
109113	3.11	7.04	49.53	0.11	0.48	0.23	3.00	0.40	4.88	0.0000018
155364	2.70	4.90	23.99	0.28	1.01	1.03	2.42	0.41	5.56	0.000000065
22040	3.11	5.65	31.96	0.37	1.13	1.28	2.73	0.40	5.45	0.000000113
140674	2.32	4.62	21.38	0.10	0.49	0.24	2.22	0.43	5.48	9.51E-08
155365	2.49	4.73	22.40	0.11	0.40	0.16	2.38	0.46	5.77	2.17E-08
140673	2.53	4.80	23.08	0.18	0.59	0.35	2.35	0.44	5.59	5.47E-08
162111	1.63	2.79	7.81	0.14	0.48	0.23	1.48	0.45	6.02	5.64E-09
14879	6.02	11.59	134.44	0.75	1.35	1.83	5.27	0.41	5.19	0.000000412
197621	2.47	5.29	28.03	0.02	0.13	0.02	2.45	0.45	5.32	0.000000218
53523	5.11	10.52	110.73	0.47	1.00	1.00	4.64	0.40	5.05	0.00000082
22039	4.62	7.91	62.58	0.60	1.27	1.62	4.02	0.44	5.77	2.14E-08
19310	2.89	6.74	45.37	0.05	0.26	0.07	2.84	0.41	4.83	0.00000224
19309	3.20	7.32	53.65	0.09	0.34	0.11	3.11	0.41	4.88	0.00000184
109111	3.43	7.47	55.76	0.18	0.66	0.43	3.25	0.40	4.98	0.00000112
53525	3.22	6.67	44.55	0.17	0.56	0.31	3.05	0.42	5.23	0.000000334
32305	6.06	12.22	149.41	0.54	1.16	1.34	5.51	0.41	5.16	0.000000475
140675	2.21	4.35	18.96	0.09	0.46	0.21	2.11	0.44	5.54	6.96E-08
32433	2.25	4.88	23.85	0.06	0.30	0.09	2.19	0.42	5.14	0.000000515
14880	5.18	10.09	101.88	0.61	1.16	1.34	4.57	0.41	5.17	0.000000446
142220	2.23	4.56	20.77	0.15	0.56	0.32	2.08	0.41	5.20	0.000000392

53524	4.61	9.66	93.27	0.39	0.96	0.91	4.22	0.40	5.00	0.00000104
33056	6.39	9.67	93.48	1.25	2.19	4.78	5.14	0.43	5.97	7.55E-09
32303	7.15	14.13	199.77	0.90	1.53	2.34	6.25	0.40	5.05	0.000000803
190943	3.78	8.71	75.82	0.03	0.23	0.05	3.75	0.42	4.95	0.0000013
162112	1.42	2.48	6.13	0.09	0.40	0.16	1.33	0.46	6.08	4.02E-09
40169	2.50	4.09	16.72	0.37	0.95	0.90	2.12	0.42	5.82	1.66E-08
190944	3.60	8.32	69.16	0.03	0.23	0.05	3.57	0.42	4.93	0.0000014
190942	3.91	9.03	81.63	0.07	0.38	0.15	3.84	0.41	4.88	0.00000184
197570	2.23	4.91	24.06	0.09	0.33	0.11	2.14	0.41	5.00	0.00000102
22768	2.94	5.67	32.12	0.34	0.82	0.67	2.60	0.40	5.21	0.000000365
140676	2.05	4.12	16.99	0.06	0.34	0.11	1.99	0.45	5.53	7.52E-08
155367	1.63	3.42	11.73	0.05	0.27	0.07	1.58	0.43	5.28	0.000000263
162113	1.35	2.42	5.84	0.09	0.40	0.16	1.26	0.45	5.90	0.000000011
14654	4.84	5.17	26.70	1.75	2.59	6.72	3.09	0.40	6.18	2.37E-09
30599	2.93	5.34	28.57	0.38	0.89	0.80	2.55	0.41	5.42	0.000000132
32304	6.65	13.30	176.76	0.74	1.33	1.77	5.91	0.40	5.08	0.000000696
140677	1.96	3.98	15.83	0.06	0.34	0.11	1.90	0.44	5.46	0.000000106
150767	4.63	7.35	54.01	0.87	1.50	2.25	3.76	0.43	5.77	2.15E-08
14878	9.01	15.32	234.83	1.59	2.44	5.98	7.42	0.42	5.50	8.98E-08
109107	3.67	7.52	56.49	0.35	0.83	0.69	3.32	0.40	5.05	0.000000828
163975	2.50	5.13	26.35	0.17	0.57	0.33	2.33	0.41	5.18	0.000000429
140678	1.88	3.87	15.01	0.06	0.34	0.11	1.82	0.43	5.38	0.000000158
30600	2.74	5.04	25.37	0.33	0.86	0.74	2.41	0.41	5.42	0.000000129
15646	2.38	4.97	24.72	0.10	0.42	0.18	2.28	0.42	5.25	0.000000312
150771	2.06	4.32	18.62	0.11	0.40	0.16	1.94	0.41	5.15	0.000000506

150770	2.13	4.45	19.81	0.13	0.41	0.17	2.00	0.41	5.14	0.000000516
62691	0.85	1.74	3.04	0.02	0.13	0.02	0.83	0.44	5.48	9.69E-08
15643	2.84	5.58	31.18	0.24	0.68	0.46	2.59	0.41	5.30	0.000000244
15645	2.44	5.02	25.22	0.11	0.43	0.18	2.32	0.43	5.30	0.000000244
35227	1.17	2.16	4.66	0.12	0.43	0.18	1.06	0.41	5.52	7.82E-08
155368	1.49	3.31	10.97	0.03	0.22	0.05	1.46	0.41	5.06	0.000000779
206115	1.86	4.34	18.85	0.04	0.26	0.07	1.82	0.40	4.82	0.00000239
162114	1.17	2.20	4.85	0.07	0.36	0.13	1.10	0.43	5.65	4.12E-08
30601	2.45	4.65	21.66	0.24	0.68	0.46	2.21	0.41	5.40	0.000000147
145032	1.32	2.85	8.11	0.06	0.27	0.07	1.26	0.40	5.07	0.000000747
145033	1.32	2.85	8.11	0.06	0.27	0.07	1.26	0.40	5.07	0.000000747
197622	1.30	3.10	9.62	0.00	0.00	0.00	1.30	0.42	4.83	0.00000231
155369	1.20	2.75	7.56	0.01	0.09	0.01	1.19	0.42	4.98	0.00000116
15644	2.66	5.42	29.33	0.20	0.61	0.37	2.46	0.41	5.18	0.000000438
140679	1.59	3.52	12.38	0.03	0.21	0.04	1.55	0.42	5.06	0.000000778
150768	3.67	6.40	40.93	0.59	1.10	1.21	3.08	0.41	5.45	0.000000114
19311	1.21	2.83	8.01	0.01	0.08	0.01	1.20	0.41	4.89	0.00000177
137612	1.00	2.25	5.05	0.03	0.17	0.03	0.97	0.40	4.93	0.00000141
162115	0.98	1.91	3.63	0.06	0.35	0.12	0.92	0.41	5.45	0.000000111
14336	1.00	2.47	6.08	0.00	0.05	0.00	1.00	0.40	4.66	0.00000501
40170	1.32	2.93	8.58	0.04	0.21	0.04	1.28	0.41	5.02	0.000000954
155370	0.92	2.30	5.29	0.00	0.00	0.00	0.92	0.40	4.61	0.00000617
184473	1.09	2.33	5.42	0.01	0.12	0.01	1.08	0.44	5.31	0.000000232
155374	1.00	2.28	5.18	0.03	0.17	0.03	0.97	0.40	4.89	0.00000169
150773	1.01	2.27	5.17	0.03	0.16	0.03	0.98	0.40	4.93	0.00000146

1154	0.51	1.04	1.08	0.01	0.12	0.02	0.50	0.43	5.44	0.000000118
137625	1.12	2.44	5.96	0.03	0.23	0.05	1.08	0.41	5.08	0.000000713
162118	0.65	1.42	2.02	0.02	0.13	0.02	0.64	0.41	5.12	0.000000576
184474	1.04	2.33	5.44	0.01	0.12	0.01	1.03	0.42	5.08	0.000000698
198323	0.61	1.34	1.79	0.01	0.12	0.01	0.60	0.41	5.10	0.000000627
198324	0.59	1.32	1.75	0.01	0.12	0.01	0.58	0.40	5.02	0.000000953
184476	0.93	2.07	4.30	0.00	0.00	0.00	0.93	0.45	5.13	0.000000562
184475	0.93	2.07	4.30	0.00	0.00	0.00	0.93	0.45	5.13	0.000000562
40171	0.88	2.21	4.89	0.00	0.00	0.00	0.88	0.40	4.56	0.000000777
1155	0.46	0.99	0.98	0.01	0.12	0.02	0.45	0.40	5.12	0.000000578
1156	0.43	0.98	0.96	0.00	0.00	0.00	0.43	0.44	5.00	0.00000102
5779	0.51	1.22	1.49	0.00	0.00	0.00	0.51	0.42	4.81	0.00000247
3658	53.29	20.69	428.12	69.25	29.20	852.48	15.96	-0.32	-5.25	0.000000307
100955	56.67	20.93	438.03	71.94	23.45	549.88	15.27	-0.34	-5.69	0.000000032
24643	44.55	18.36	337.21	58.01	20.99	440.39	13.46	-0.34	-5.66	3.86E-08
24644	38.41	16.60	275.56	49.85	18.83	354.40	11.44	-0.32	-5.35	0.000000191
75322	26.92	11.93	142.35	35.68	14.41	207.75	8.76	-0.33	-5.49	9.04E-08
100957	50.67	19.48	379.37	64.09	21.46	460.40	13.42	-0.33	-5.43	0.000000127
75321	31.06	13.85	191.80	41.76	16.50	272.27	10.70	-0.35	-5.83	1.59E-08
189313	46.04	18.20	331.30	58.67	22.25	495.28	12.63	-0.31	-5.16	0.000000481
100956	53.52	19.99	399.59	67.64	22.02	484.81	14.13	-0.34	-5.57	6.23E-08
174999	44.89	21.78	474.29	59.67	24.47	598.63	14.78	-0.32	-5.29	0.000000253
9374	46.19	23.41	547.98	63.85	30.59	935.98	17.66	-0.33	-5.39	0.000000155
24639	90.58	30.57	934.59	114.08	36.08	1301.54	23.50	-0.35	-5.83	1.56E-08
180703	113.51	30.34	920.29	136.50	36.19	1309.92	22.99	-0.35	-5.71	2.92E-08

100954	63.74	21.14	447.02	80.53	26.57	705.87	16.78	-0.35	-5.81	1.78E-08
125190	63.03	20.51	420.81	77.88	24.07	579.44	14.85	-0.33	-5.51	8.39E-08
54573	27.32	11.84	140.27	37.02	18.73	350.98	9.70	-0.32	-5.16	0.000000478
9375	40.96	20.80	432.82	56.32	27.76	770.80	15.36	-0.32	-5.21	0.00000038
114431	79.97	36.88	1360.41	104.13	42.48	1804.56	24.16	-0.30	-5.04	0.000000863
180704	109.89	30.10	906.19	131.53	35.10	1232.17	21.64	-0.33	-5.49	9.28E-08
180705	100.65	27.37	749.21	121.40	32.82	1076.95	20.75	-0.34	-5.70	3.12E-08
75318	40.28	15.74	247.59	53.41	19.82	392.81	13.12	-0.37	-6.09	3.8E-09
7577	35.25	15.09	227.74	49.22	25.23	636.68	13.97	-0.35	-5.61	5.05E-08
116026	18.14	9.36	87.66	25.61	14.01	196.37	7.47	-0.32	-5.22	0.000000348
125191	54.37	17.66	311.87	65.92	20.52	421.27	11.55	-0.30	-5.00	0.00000102
75320	33.38	14.31	204.76	45.00	17.91	320.61	11.62	-0.36	-5.96	7.96E-09
17992	35.92	13.87	192.37	45.56	17.31	299.63	9.64	-0.31	-5.11	0.00000062
7575	74.01	22.56	509.15	97.82	41.19	1696.52	23.81	-0.37	-5.99	6.64E-09
24642	56.23	21.82	476.14	72.91	26.22	687.25	16.68	-0.35	-5.74	2.53E-08
100953	67.69	21.74	472.41	84.82	28.43	808.43	17.13	-0.34	-5.62	4.62E-08
75319	36.83	15.58	242.78	49.73	19.26	370.79	12.89	-0.37	-6.11	3.39E-09
126874	20.55	11.69	136.55	28.76	15.73	247.45	8.21	-0.30	-4.93	0.00000145
203525	98.26	33.40	1115.60	120.27	35.66	1271.57	22.01	-0.32	-5.28	0.00000027
24640	86.67	28.94	837.78	109.02	34.69	1203.51	22.35	-0.35	-5.81	1.78E-08
78188	120.67	41.09	1688.18	150.03	47.41	2247.34	29.36	-0.33	-5.49	9.24E-08
24641	61.55	22.93	525.76	78.99	27.43	752.55	17.44	-0.35	-5.72	2.73E-08
27300	25.23	14.09	198.45	35.05	17.21	296.23	9.82	-0.31	-5.18	0.000000427
36304	204.85	71.46	5106.14	252.14	81.36	6620.09	47.29	-0.31	-5.12	0.000000577
75616	57.27	22.57	509.22	71.12	22.96	527.34	13.85	-0.30	-5.03	0.000000878

171893	36.57	20.32	413.02	53.67	32.34	1045.99	17.09	-0.32	-5.28	0.000000269
126871	126.99	46.97	2205.83	161.17	66.11	4370.85	34.19	-0.30	-4.96	0.00000124
97256	29.19	10.41	108.39	36.85	14.78	218.56	7.66	-0.30	-4.99	0.00000109
54574	16.83	7.85	61.70	23.53	14.22	202.29	6.70	-0.30	-4.87	0.00000188
36303	215.85	75.75	5738.04	265.03	86.63	7504.95	49.17	-0.30	-5.01	0.00000098
202311	137.84	55.34	3062.27	176.45	69.77	4867.47	38.61	-0.31	-5.09	0.000000658
99171	115.43	36.89	1360.67	142.46	47.42	2248.90	27.03	-0.32	-5.29	0.000000256
126873	102.93	39.41	1553.00	132.18	57.30	3282.84	29.25	-0.30	-4.95	0.00000129
7576	68.95	21.59	466.10	90.84	37.33	1393.48	21.89	-0.37	-5.99	6.53E-09
7701	207.57	78.54	6168.45	261.10	89.26	7966.58	53.52	-0.32	-5.28	0.000000267
7574	84.47	24.29	589.99	110.74	42.92	1842.44	26.27	-0.39	-6.29	1.26E-09
149453	88.94	41.07	1687.05	120.11	62.01	3845.52	31.18	-0.30	-4.94	0.00000138
7573	124.14	35.50	1260.17	155.61	57.84	3345.17	31.47	-0.34	-5.47	0.000000102
78187	136.58	48.10	2313.91	168.10	55.32	3060.54	31.52	-0.30	-5.04	0.000000841
99172	112.99	36.18	1308.69	139.27	46.24	2138.56	26.29	-0.32	-5.26	0.000000292
75129	66.63	20.61	424.61	83.95	36.22	1311.88	17.31	-0.30	-4.91	0.00000016
126872	118.73	45.14	2037.74	151.79	64.11	4110.58	33.06	-0.30	-4.96	0.00000123
99173	110.07	35.55	1263.93	135.45	45.06	2030.20	25.37	-0.31	-5.19	0.000000405
90819	22.99	14.38	206.90	32.32	16.62	276.15	9.34	-0.30	-4.98	0.00000112
74073	56.83	22.93	525.81	74.39	35.46	1257.60	17.56	-0.30	-4.90	0.00000164
62822	130.58	42.92	1842.46	162.93	51.49	2651.32	32.34	-0.34	-5.66	3.79E-08
7700	221.23	83.49	6971.20	277.17	94.18	8868.98	55.94	-0.31	-5.21	0.000000372
89080	97.17	39.20	1536.28	123.58	48.16	2318.99	26.41	-0.30	-4.99	0.00000106
36305	196.88	69.33	4806.14	241.40	78.51	6163.68	44.52	-0.30	-4.98	0.00000112
160627	32.38	15.87	251.98	42.48	17.57	308.76	10.10	-0.30	-5.00	0.00000105

9376	12.32	8.75	76.58	19.37	14.50	210.30	7.05	-0.30	-4.91	0.00000155
7699	239.20	90.37	8165.86	298.27	101.59	10319.95	59.07	-0.31	-5.09	0.00000066
123337	67.43	21.73	472.40	81.75	25.45	647.94	14.32	-0.30	-5.02	0.000000942
7703	58.65	27.01	729.40	76.61	28.75	826.66	17.96	-0.32	-5.33	0.000000204
57404	15.38	8.31	69.00	21.99	12.31	151.58	6.60	-0.32	-5.24	0.000000327
35413	99.38	44.16	1950.22	128.07	46.68	2179.30	28.69	-0.32	-5.23	0.000000343
90817	126.62	40.55	1644.33	153.63	47.74	2279.41	27.02	-0.31	-5.06	0.000000772
133220	168.67	54.24	2942.33	205.88	67.56	4564.54	37.21	-0.31	-5.04	0.000000836
127235	71.38	26.43	698.47	87.54	26.98	728.05	16.16	-0.30	-5.01	0.000000999
18002	87.35	32.39	1049.01	110.10	40.66	1653.55	22.75	-0.31	-5.14	0.000000524
17680	34.38	11.44	130.85	43.56	17.65	311.68	9.19	-0.32	-5.15	0.000000508
202310	146.77	58.37	3406.96	187.92	74.60	5564.67	41.15	-0.31	-5.10	0.000000625
113054	50.69	23.12	534.45	65.46	24.63	606.52	14.78	-0.31	-5.12	0.00000057
58323	29.22	14.18	201.15	38.91	18.02	324.67	9.69	-0.30	-4.97	0.00000121
75317	46.30	17.75	315.05	59.71	22.80	519.78	13.41	-0.33	-5.45	0.000000112
90224	48.01	16.82	282.85	60.08	23.00	529.00	12.07	-0.30	-4.98	0.00000111
78181	92.58	26.43	698.64	111.35	33.60	1129.18	18.77	-0.31	-5.16	0.000000482
30580	58.66	23.94	573.34	77.68	36.40	1325.28	19.02	-0.32	-5.14	0.000000517
116025	46.43	17.72	313.98	59.85	25.65	657.74	13.42	-0.31	-5.07	0.000000743
35412	200.32	86.76	7527.10	259.22	91.15	8308.53	58.90	-0.33	-5.48	9.69E-08
35411	232.14	98.92	9784.26	298.92	112.34	12619.23	66.78	-0.32	-5.23	0.000000338
35414	97.62	43.56	1897.58	125.24	45.83	2100.49	27.63	-0.31	-5.12	0.000000593
202309	172.12	67.28	4526.42	218.42	86.71	7519.47	46.30	-0.30	-4.96	0.00000126
123336	89.67	26.30	691.84	107.95	34.19	1169.23	18.28	-0.30	-4.98	0.00000112
24632	70.50	27.40	751.01	87.30	28.59	817.67	16.80	-0.30	-4.97	0.00000121

189312	101.85	31.50	992.23	123.62	37.10	1376.40	21.76	-0.32	-5.25	0.000000312
24631	96.48	37.11	1376.89	120.51	40.74	1659.38	24.03	-0.31	-5.11	0.000000607
41489	146.28	44.66	1994.81	176.32	51.76	2679.09	30.04	-0.31	-5.15	0.000000492
54571	40.44	16.11	259.45	52.38	22.94	526.42	11.94	-0.31	-5.01	0.000000972
24476	92.17	30.90	954.83	116.80	45.61	2080.37	24.62	-0.32	-5.26	0.000000287
54570	42.23	16.65	277.34	54.50	23.87	569.58	12.26	-0.30	-4.96	0.00000124
84787	59.56	20.54	422.09	73.64	25.56	653.18	14.08	-0.31	-5.04	0.000000838
41491	139.96	42.97	1846.28	167.72	49.43	2443.74	27.76	-0.30	-4.97	0.00000118
204581	26.89	11.63	135.33	36.01	18.69	349.35	9.13	-0.30	-4.89	0.00000174
41490	142.69	43.54	1895.43	171.00	50.69	2569.58	28.31	-0.30	-4.97	0.00000119
54572	33.59	13.40	179.59	44.31	20.83	434.02	10.72	-0.31	-5.10	0.000000631
30581	51.49	21.87	478.33	68.48	31.24	975.66	17.00	-0.32	-5.25	0.000000311

Supplementary Table 3: Performance of single features of Top 100 positively and bottom 100 negatively correlated Methylated sites(from 30791 MS)

Top 100 Positively correlated methylation sites											
Site ID	Mean_ CRC	Mean_ NOR	Threshold	True Positive	True Negative	False Positive	False Negative	Sensitivity	Specificity	FPR	AUC-ROC
181489	5.27	0.63	0.63	103	102	30	39	0.73	0.77	0.23	0.75
196741	6.48	0.50	0.50	93	109	23	49	0.65	0.83	0.17	0.74
196742	6.15	0.37	0.37	88	113	19	54	0.62	0.86	0.14	0.74
181490	4.38	0.38	0.38	90	111	21	52	0.63	0.84	0.16	0.74
181491	3.33	0.12	0.48	74	124	8	68	0.52	0.94	0.06	0.73
93487	3.33	0.15	0.15	75	120	12	67	0.53	0.91	0.09	0.72
38139	7.06	0.61	0.61	100	96	36	42	0.70	0.73	0.27	0.72

86829	3.96	0.61	0.98	92	103	29	50	0.65	0.78	0.22	0.71
189090	3.00	0.61	0.61	93	101	31	49	0.65	0.77	0.23	0.71
164637	3.00	0.12	0.44	68	124	8	74	0.48	0.94	0.06	0.71
197569	2.47	0.13	0.39	71	120	12	71	0.50	0.91	0.09	0.70
33055	10.08	2.46	3.31	95	97	35	47	0.67	0.73	0.27	0.70
19308	3.39	0.09	0.46	67	123	9	75	0.47	0.93	0.07	0.70
155363	2.85	0.34	0.62	76	114	18	66	0.54	0.86	0.14	0.70
93488	2.98	0.08	0.72	63	126	6	79	0.44	0.95	0.05	0.70
19307	4.02	0.38	0.38	85	105	27	57	0.60	0.80	0.20	0.70
155366	2.45	0.10	0.62	64	124	8	78	0.45	0.94	0.06	0.70
164638	2.70	0.11	0.40	64	124	8	78	0.45	0.94	0.06	0.70
109113	3.11	0.11	0.44	64	124	8	78	0.45	0.94	0.06	0.70
155364	2.70	0.28	0.28	72	116	16	70	0.51	0.88	0.12	0.69
22040	3.10	0.37	0.37	75	113	19	67	0.53	0.86	0.14	0.69
140674	2.32	0.10	0.35	61	126	6	81	0.43	0.95	0.05	0.69
155365	2.49	0.11	0.64	64	123	9	78	0.45	0.93	0.07	0.69
140673	2.53	0.18	0.44	67	120	12	75	0.47	0.91	0.09	0.69
162111	1.63	0.14	0.47	68	119	13	74	0.48	0.90	0.10	0.69
14879	6.02	0.75	0.75	98	91	41	44	0.69	0.69	0.31	0.69
197621	2.47	0.02	0.29	56	130	2	86	0.39	0.98	0.02	0.69
53523	5.11	0.47	0.47	87	101	31	55	0.61	0.77	0.23	0.69
22039	4.62	0.60	0.60	88	100	32	54	0.62	0.76	0.24	0.69
19310	2.89	0.05	0.68	60	126	6	82	0.42	0.95	0.05	0.69
19309	3.20	0.09	0.44	63	123	9	79	0.44	0.93	0.07	0.69
109111	3.43	0.18	0.54	65	121	11	77	0.46	0.92	0.08	0.69
53525	3.22	0.17	0.17	67	119	13	75	0.47	0.90	0.10	0.69

32305	6.06	0.54	0.54	84	103	29	58	0.59	0.78	0.22	0.69
140675	2.21	0.09	0.33	59	126	6	83	0.42	0.95	0.05	0.69
32433	2.25	0.06	0.55	59	126	6	83	0.42	0.95	0.05	0.69
14880	5.18	0.61	0.61	92	95	37	50	0.65	0.72	0.28	0.68
142220	2.23	0.15	0.38	64	121	11	78	0.45	0.92	0.08	0.68
53524	4.61	0.39	0.39	79	107	25	63	0.56	0.81	0.19	0.68
33056	6.39	1.25	1.25	95	92	40	47	0.67	0.70	0.30	0.68
32303	7.15	0.90	0.90	95	92	40	47	0.67	0.70	0.30	0.68
190943	3.78	0.03	0.45	55	129	3	87	0.39	0.98	0.02	0.68
162112	1.42	0.09	0.39	60	124	8	82	0.42	0.94	0.06	0.68
40169	2.50	0.37	0.61	76	109	23	66	0.54	0.83	0.17	0.68
190944	3.60	0.03	0.82	53	130	2	89	0.37	0.98	0.02	0.68
190942	3.91	0.07	0.50	56	127	5	86	0.39	0.96	0.04	0.68
197570	2.23	0.09	0.57	61	122	10	81	0.43	0.92	0.08	0.68
22768	2.94	0.34	0.34	77	107	25	65	0.54	0.81	0.19	0.68
140676	2.05	0.06	0.50	55	127	5	87	0.39	0.96	0.04	0.67
155367	1.63	0.05	0.40	55	127	5	87	0.39	0.96	0.04	0.67
162113	1.35	0.09	0.37	58	124	8	84	0.41	0.94	0.06	0.67
14654	4.84	1.75	3.47	74	109	23	68	0.52	0.83	0.17	0.67
30599	2.93	0.38	0.38	77	106	26	65	0.54	0.80	0.20	0.67
32304	6.65	0.74	0.74	93	91	41	49	0.65	0.69	0.31	0.67
140677	1.96	0.06	0.48	54	127	5	88	0.38	0.96	0.04	0.67
150767	4.63	0.87	0.87	98	86	46	44	0.69	0.65	0.35	0.67
14878	9.01	1.59	3.24	70	112	20	72	0.49	0.85	0.15	0.67
109107	3.67	0.35	0.72	73	109	23	69	0.51	0.83	0.17	0.67
163975	2.50	0.17	0.43	62	118	14	80	0.44	0.89	0.11	0.67

140678	1.88	0.06	0.46	52	127	5	90	0.37	0.96	0.04	0.66
30600	2.74	0.33	0.33	69	111	21	73	0.49	0.84	0.16	0.66
15646	2.38	0.10	0.35	56	123	9	86	0.39	0.93	0.07	0.66
150771	2.06	0.11	0.33	60	119	13	82	0.42	0.90	0.10	0.66
150770	2.13	0.13	0.35	61	118	14	81	0.43	0.89	0.11	0.66
62691	0.85	0.02	0.48	49	129	3	93	0.35	0.98	0.02	0.66
15643	2.84	0.24	0.53	65	114	18	77	0.46	0.86	0.14	0.66
15645	2.44	0.11	0.37	56	122	10	86	0.39	0.92	0.08	0.66
35227	1.17	0.12	0.47	56	122	10	86	0.39	0.92	0.08	0.66
155368	1.49	0.03	0.35	48	129	3	94	0.34	0.98	0.02	0.66
206115	1.86	0.04	0.44	48	129	3	94	0.34	0.98	0.02	0.66
162114	1.17	0.07	0.44	52	125	7	90	0.37	0.95	0.05	0.66
30601	2.45	0.24	0.24	61	116	16	81	0.43	0.88	0.12	0.65
145032	1.32	0.06	0.62	50	126	6	92	0.35	0.95	0.05	0.65
145033	1.32	0.06	0.62	50	126	6	92	0.35	0.95	0.05	0.65
197622	1.30	0.00	0.43	43	132	0	99	0.30	1.00	0.00	0.65
155369	1.20	0.01	0.41	44	131	1	98	0.31	0.99	0.01	0.65
15644	2.66	0.20	0.47	61	115	17	81	0.43	0.87	0.13	0.65
140679	1.59	0.03	0.55	47	128	4	95	0.33	0.97	0.03	0.65
150768	3.67	0.59	0.93	80	97	35	62	0.56	0.73	0.27	0.65
19311	1.21	0.01	0.54	43	131	1	99	0.30	0.99	0.01	0.65
137612	1.00	0.03	0.57	45	129	3	97	0.32	0.98	0.02	0.65
162115	0.98	0.06	0.47	46	127	5	96	0.32	0.96	0.04	0.64
14336	1.00	0.00	0.44	41	131	1	101	0.29	0.99	0.01	0.64
40170	1.32	0.04	0.47	44	128	4	98	0.31	0.97	0.03	0.64
155370	0.92	0.00	0.41	39	132	0	103	0.27	1.00	0.00	0.64

184473	1.09	0.01	0.37	40	131	1	102	0.28	0.99	0.01	0.64
155374	1.00	0.03	0.78	41	130	2	101	0.29	0.98	0.02	0.64
150773	1.01	0.03	0.47	43	127	5	99	0.30	0.96	0.04	0.63
1154	0.51	0.01	0.45	37	131	1	105	0.26	0.99	0.01	0.63
137625	1.12	0.03	0.51	39	129	3	103	0.27	0.98	0.02	0.63
162118	0.65	0.02	0.58	37	130	2	105	0.26	0.98	0.02	0.62
184474	1.04	0.01	0.47	35	131	1	107	0.25	0.99	0.01	0.62
198323	0.61	0.01	0.61	36	130	2	106	0.25	0.98	0.02	0.62
198324	0.59	0.01	0.59	36	130	2	106	0.25	0.98	0.02	0.62
184476	0.93	0.00	0.52	33	132	0	109	0.23	1.00	0.00	0.62
184475	0.93	0.00	0.52	33	132	0	109	0.23	1.00	0.00	0.62
40171	0.88	0.00	0.49	33	132	0	109	0.23	1.00	0.00	0.62
1155	0.46	0.01	0.46	34	131	1	108	0.24	0.99	0.01	0.62
1156	0.43	0.00	0.43	31	132	0	111	0.22	1.00	0.00	0.61
5779	0.51	0.00	0.45	31	132	0	111	0.22	1.00	0.00	0.61

Top 100 Negatively correlated methylation sites											
Site ID	Mean_ CRC	Mean_ NOR	Threshold	True Positive	True Negative	False Positive	False Negative	Sensitivity	Specificity	FPR	AUC- ROC
3658	53.29	69.25	61.27	106	79	53	36	0.75	0.60	0.40	0.67
100955	56.67	71.94	64.31	105	79	53	37	0.74	0.60	0.40	0.67
24643	44.55	58.01	51.28	102	81	51	40	0.72	0.61	0.39	0.67
24644	38.41	49.85	44.13	99	83	49	43	0.70	0.63	0.37	0.66
75322	26.92	35.68	31.30	103	79	53	39	0.73	0.60	0.40	0.66
100957	50.67	64.09	57.38	103	79	53	39	0.73	0.60	0.40	0.66

75321	31.06	41.76	36.41	106	76	56	36	0.75	0.58	0.42	0.66
189313	46.04	58.67	52.36	102	79	53	40	0.72	0.60	0.40	0.66
100956	53.52	67.64	60.58	103	78	54	39	0.73	0.59	0.41	0.66
174999	44.89	59.67	52.28	104	77	55	38	0.73	0.58	0.42	0.66
9374	46.19	63.85	55.02	110	71	61	32	0.77	0.54	0.46	0.66
24639	90.58	114.08	102.33	100	80	52	42	0.70	0.61	0.39	0.66
180703	113.51	136.50	125.00	100	80	52	42	0.70	0.61	0.39	0.66
100954	63.74	80.53	72.14	102	78	54	40	0.72	0.59	0.41	0.65
125190	63.03	77.88	70.46	103	77	55	39	0.73	0.58	0.42	0.65
54573	27.32	37.02	32.17	103	77	55	39	0.73	0.58	0.42	0.65
9375	40.96	56.32	48.64	110	70	62	32	0.77	0.53	0.47	0.65
114431	79.97	104.13	92.05	98	81	51	44	0.69	0.61	0.39	0.65
180704	109.89	131.53	120.71	100	79	53	42	0.70	0.60	0.40	0.65
180705	100.65	121.40	111.02	101	78	54	41	0.71	0.59	0.41	0.65
75318	40.28	53.41	46.84	104	75	57	38	0.73	0.57	0.43	0.65
7577	35.25	49.22	42.24	105	74	58	37	0.74	0.56	0.44	0.65
116026	18.14	25.61	21.88	103	75	57	39	0.73	0.57	0.43	0.65
125191	54.37	65.92	60.14	103	75	57	39	0.73	0.57	0.43	0.65
75320	33.38	45.00	39.19	104	74	58	38	0.73	0.56	0.44	0.65
17992	35.92	45.56	40.74	94	83	49	48	0.66	0.63	0.37	0.65
7575	74.01	97.82	85.92	97	80	52	45	0.68	0.61	0.39	0.64
24642	56.23	72.91	64.57	98	79	53	44	0.69	0.60	0.40	0.64
100953	67.69	84.82	76.26	101	76	56	41	0.71	0.58	0.42	0.64
75319	36.83	49.73	43.28	102	75	57	40	0.72	0.57	0.43	0.64
126874	20.55	28.76	24.66	104	73	59	38	0.73	0.55	0.45	0.64
203525	98.26	120.27	109.26	95	81	51	47	0.67	0.61	0.39	0.64

24640	86.67	109.02	97.84	98	78	54	44	0.69	0.59	0.41	0.64
78188	120.67	150.03	135.35	99	77	55	43	0.70	0.58	0.42	0.64
24641	61.55	78.99	70.27	100	76	56	42	0.70	0.58	0.42	0.64
27300	25.23	35.05	30.14	105	71	61	37	0.74	0.54	0.46	0.64
36304	204.85	252.14	228.50	96	79	53	46	0.68	0.60	0.40	0.64
75616	57.27	71.12	64.20	96	79	53	46	0.68	0.60	0.40	0.64
171893	36.57	53.67	45.12	100	75	57	42	0.70	0.57	0.43	0.64
126871	126.99	161.17	144.08	100	75	57	42	0.70	0.57	0.43	0.64
97256	29.19	36.85	33.02	94	80	52	48	0.66	0.61	0.39	0.63
54574	16.83	23.53	20.18	103	71	61	39	0.73	0.54	0.46	0.63
36303	215.85	265.03	240.44	96	77	55	46	0.68	0.58	0.42	0.63
202311	137.84	176.45	157.14	99	74	58	43	0.70	0.56	0.44	0.63
99171	115.43	142.46	128.94	100	73	59	42	0.70	0.55	0.45	0.63
126873	102.93	132.18	117.56	100	73	59	42	0.70	0.55	0.45	0.63
7576	68.95	90.84	79.90	91	81	51	51	0.64	0.61	0.39	0.63
7701	207.57	261.10	234.34	92	80	52	50	0.65	0.61	0.39	0.63
7574	84.47	110.74	97.60	93	79	53	49	0.65	0.60	0.40	0.63
149453	88.94	120.11	104.52	93	79	53	49	0.65	0.60	0.40	0.63
7573	124.14	155.61	139.88	96	76	56	46	0.68	0.58	0.42	0.63
78187	136.58	168.10	152.34	97	75	57	45	0.68	0.57	0.43	0.63
99172	112.99	139.27	126.13	99	73	59	43	0.70	0.55	0.45	0.63
75129	66.63	83.94	75.28	99	73	59	43	0.70	0.55	0.45	0.63
126872	118.73	151.79	135.26	99	73	59	43	0.70	0.55	0.45	0.63
99173	110.07	135.45	122.76	100	72	60	42	0.70	0.55	0.45	0.62
90819	22.99	32.32	27.66	100	72	60	42	0.70	0.55	0.45	0.62
74073	56.83	74.39	65.61	103	69	63	39	0.73	0.52	0.48	0.62

62822	130.58	162.93	146.76	93	78	54	49	0.65	0.59	0.41	0.62
7700	221.23	277.17	249.20	93	78	54	49	0.65	0.59	0.41	0.62
89080	97.17	123.58	110.38	93	78	54	49	0.65	0.59	0.41	0.62
36305	196.88	241.40	219.14	97	74	58	45	0.68	0.56	0.44	0.62
160627	32.38	42.48	37.43	99	72	60	43	0.70	0.55	0.45	0.62
9376	12.32	19.37	15.84	103	68	64	39	0.73	0.52	0.48	0.62
7699	239.20	298.27	268.74	94	76	56	48	0.66	0.58	0.42	0.62
123337	67.43	81.75	74.59	94	76	56	48	0.66	0.58	0.42	0.62
7703	58.65	76.61	67.63	95	75	57	47	0.67	0.57	0.43	0.62
57404	15.38	21.99	18.68	96	74	58	46	0.68	0.56	0.44	0.62
35413	99.38	128.07	113.72	96	74	58	46	0.68	0.56	0.44	0.62
90817	126.62	153.63	140.12	96	74	58	46	0.68	0.56	0.44	0.62
133220	168.67	205.88	187.27	97	73	59	45	0.68	0.55	0.45	0.62
127235	71.38	87.54	79.46	97	73	59	45	0.68	0.55	0.45	0.62
18002	87.35	110.10	98.72	98	72	60	44	0.69	0.55	0.45	0.62
17680	34.38	43.56	38.97	94	75	57	48	0.66	0.57	0.43	0.62
202310	146.77	187.92	167.34	94	75	57	48	0.66	0.57	0.43	0.62
113054	50.69	65.46	58.08	95	74	58	47	0.67	0.56	0.44	0.61
58323	29.22	38.91	34.06	95	74	58	47	0.67	0.56	0.44	0.61
75317	46.30	59.71	53.00	97	72	60	45	0.68	0.55	0.45	0.61
90224	48.01	60.08	54.04	97	72	60	45	0.68	0.55	0.45	0.61
78181	92.58	111.35	101.96	98	71	61	44	0.69	0.54	0.46	0.61
30580	58.66	77.68	68.17	100	69	63	42	0.70	0.52	0.48	0.61
116025	46.43	59.85	53.14	93	75	57	49	0.65	0.57	0.43	0.61
35412	200.32	259.22	229.77	95	73	59	47	0.67	0.55	0.45	0.61
35411	232.14	298.92	265.53	95	73	59	47	0.67	0.55	0.45	0.61

35414	97.62	125.24	111.43	95	73	59	47	0.67	0.55	0.45	0.61
202309	172.12	218.42	195.27	95	73	59	47	0.67	0.55	0.45	0.61
123336	89.67	107.95	98.81	95	72	60	47	0.67	0.55	0.45	0.61
24632	70.50	87.30	78.90	88	78	54	54	0.62	0.59	0.41	0.61
189312	101.85	123.62	112.74	89	77	55	53	0.63	0.58	0.42	0.61
24631	96.48	120.51	108.50	91	75	57	51	0.64	0.57	0.43	0.60
41489	146.28	176.32	161.30	94	71	61	48	0.66	0.54	0.46	0.60
54571	40.44	52.38	46.41	95	70	62	47	0.67	0.53	0.47	0.60
24476	92.17	116.80	104.48	92	72	60	50	0.65	0.55	0.45	0.60
54570	42.23	54.50	48.36	92	72	60	50	0.65	0.55	0.45	0.60
84787	59.56	73.64	66.60	93	71	61	49	0.65	0.54	0.46	0.60
41491	139.96	167.72	153.84	94	70	62	48	0.66	0.53	0.47	0.60
204581	26.89	36.01	31.45	97	67	65	45	0.68	0.51	0.49	0.60
41490	142.69	171.00	156.84	92	71	61	50	0.65	0.54	0.46	0.59
54572	33.59	44.31	38.95	95	68	64	47	0.67	0.52	0.48	0.59
30581	51.49	68.48	59.98	101	62	70	41	0.71	0.47	0.53	0.59

Supplementary Table 4: Performance of the Machine learning model built on 30791 methylated sites.

Model Name	Thr	TPR	FPR	YC	Training							Validation Set						
					Sp	Sn	AUC	Acc	Pre	MC	K	Sp	Sn	AUC	Acc	Pre	MC	K
SVC	0.66	0.48	0.07	0.41	71.43	69.57	0.71	70.45	72.73	0.41	0.41	92.86	48.15	0.71	70.91	86.67	0.46	0.41
Logistic Regression	0.61	0.85	0.18	0.67	80.95	65.22	0.73	72.73	78.95	0.47	0.46	82.14	85.19	0.84	83.64	82.14	0.67	0.67
Naive Bayes	1.00	1.00	0.86	0.14	30.00	95.65	0.63	65.12	61.11	0.35	0.27	14.29	100.00	0.57	56.36	52.94	0.28	0.14
Decision Tree	1.00	0.78	0.39	0.38	71.43	65.22	0.68	68.18	71.43	0.37	0.36	60.71	77.78	0.69	69.09	65.63	0.39	0.38

Random Forest	0.54	0.89	0.18	0.71	76.19	82.61	0.79	79.55	79.17	0.59	0.59	82.14	88.89	0.86	85.45	82.76	0.71	0.71
Extra Trees	0.51	0.93	0.18	0.75	70.00	69.57	0.70	69.77	72.73	0.39	0.39	82.14	92.59	0.87	87.27	83.33	0.75	0.75
AdaBoost	0.50	0.93	0.18	0.75	85.71	86.96	0.86	86.36	86.96	0.73	0.73	82.14	92.59	0.87	87.27	83.33	0.75	0.75
Gradient Boosting	0.57	0.85	0.11	0.74	80.95	82.61	0.82	81.82	82.61	0.64	0.64	89.29	85.19	0.87	87.27	88.46	0.75	0.75
Multiple Layer Perceptron	1.00	0.70	0.04	0.67	70.00	69.57	0.70	69.77	72.73	0.39	0.39	96.43	70.37	0.83	83.64	95.00	0.69	0.67
XGBoost	0.17	0.96	0.36	0.61	75.00	69.57	0.72	72.09	76.19	0.44	0.44	64.29	96.30	0.80	80.00	72.22	0.64	0.60

#Thr: Threshold; YC: Youden Coeff; Sp: Specificity; Sn: Sensitivity; Acc: Accuracy; Pre: Precision; MC: Mathews Coeff; K :Kappa

Supplementary Table 5.1: List of selected features based on Univariate analysis for positively and negatively correlated Methylated sites

Positive_Top_25_M S	Positive_Top_15_ MS	Positive_Top_5_ MS	Negative_Top_5_ MS	Negative_Top_15_ MS	Negative_Top_25_ MS
19307	19308	181489	24642	3658	3658
19308	33055	181490	24643	9374	7576
22040	38139	181491	100955	24641	9374
33055	86829	196741	100956	24642	9375
38139	93487	196742	100957	24643	17992
86829	93488			36303	24639
93487	155363			36304	24641
93488	164637			75319	24642
109113	181489			100953	24643
140673	181490			100954	24644
140674	181491			100955	36303
155363	189090			100956	36304

155364	196741			100957	36305
155365	196742			180703	54573
155366	197569			189313	75318
162111					75319
164637					100953
164638					100954
181489					100955
181490					100956
181491					100957
189090					180703
196741					180704
196742					180705
197569					189313

Supplementary Table 5.2: ML Performance of Univariate selected feature sets on Top 100 positively and negatively Correlated Methylated sites

Positively_Corr_25_performance_metrics											
Name	Thresh	Training					Validation				
		Sens	Spec	Acc	AUC	MCC	Sens	Spec	Acc	AUC	MCC
RF	0.51	75.68	75.93	75.80	0.86	0.52	80.65	70.83	76.36	0.87	0.52
LR	0.42	77.48	77.78	77.63	0.88	0.55	83.87	79.17	81.82	0.87	0.63
MLP	0.46	76.58	75.93	76.26	0.84	0.53	90.32	66.67	80.00	0.87	0.59
XGB	0.53	73.87	74.07	73.97	0.82	0.48	83.87	66.67	76.36	0.83	0.52
KN	0.60	71.17	84.26	77.63	0.84	0.56	64.52	70.83	67.27	0.75	0.35
ET	0.51	76.58	75.93	76.26	0.86	0.53	90.32	70.83	81.82	0.88	0.63

Positively_Corr_15_performance_metrics											
Name	Thresh	Training					Validation				
		Sens	Spec	Acc	AUC	MCC	Sens	Spec	Acc	AUC	MCC
RF	0.51	78.38	78.70	78.54	0.85	0.57	80.65	66.67	74.55	0.86	0.48
LR	0.42	79.28	79.63	79.45	0.88	0.59	83.87	79.17	81.82	0.88	0.63
MLP	0.46	76.58	75.93	76.26	0.83	0.53	87.10	70.83	80.00	0.86	0.59
XGB	0.35	74.78	75.00	74.89	0.84	0.50	87.10	62.50	76.36	0.84	0.52
KN	0.60	77.48	82.41	79.91	0.86	0.60	74.19	66.67	70.91	0.76	0.41
ET	0.52	77.48	75.93	76.71	0.85	0.53	87.10	58.33	74.55	0.88	0.48

Positively_Corr_5_performance_metrics											
Name	Thresh	Training					Validation				
		Sens	Spec	Acc	AUC	MCC	Sens	Spec	Acc	AUC	MCC
RF	0.35	80.18	80.56	80.37	0.83	0.61	80.65	79.17	80.00	0.76	0.60
LR	0.33	75.68	75.93	75.80	0.80	0.52	74.19	58.33	67.27	0.81	0.33
MLP	0.40	77.48	76.85	77.17	0.82	0.54	83.87	66.67	76.36	0.86	0.52
XGB	0.28	75.68	79.63	77.63	0.79	0.55	80.65	79.17	80.00	0.76	0.60
KN	0.60	73.87	80.56	77.17	0.83	0.55	67.74	79.17	72.73	0.80	0.47
ET	0.28	81.08	81.48	81.28	0.84	0.63	80.65	79.17	80.00	0.74	0.60

Negatively_Corr_25_performance_metrics											
Name	Thresh	Training					Validation				
		Sens	Spec	Acc	AUC	MCC	Sens	Spec	Acc	AUC	MCC
RF	0.49	71.17	69.44	70.32	0.78	0.41	80.65	50.00	67.27	0.69	0.32
LR	0.47	61.26	61.11	61.19	0.60	0.22	48.39	45.83	47.27	0.43	-0.06

MLP	0.46	52.25	51.85	52.06	0.55	0.04	41.94	66.67	52.73	0.51	0.09
XGB	0.56	68.47	68.52	68.49	0.75	0.37	61.29	58.33	60.00	0.67	0.20
KN	0.60	76.58	72.22	74.43	0.76	0.49	80.65	58.33	70.91	0.70	0.40
ET	0.50	73.87	74.07	73.97	0.78	0.48	83.87	54.17	70.91	0.74	0.40

Negatively_Corr_15_performance_metrics											
		Training					Validation				
Name	Thresh	Sens	Spec	Acc	AUC	MCC	Sens	Spec	Acc	AUC	MCC
RF	0.48	66.67	66.67	66.67	0.75	0.33	80.65	58.33	70.91	0.69	0.40
LR	0.47	61.26	62.96	62.10	0.66	0.24	64.52	41.67	54.55	0.52	0.06
MLP	0.48	51.35	50.00	50.69	0.56	0.01	48.39	70.83	58.18	0.66	0.20
XGB	0.41	67.57	67.59	67.58	0.74	0.35	74.19	54.17	65.46	0.65	0.29
KN	0.60	71.17	67.59	69.41	0.74	0.39	70.97	54.17	63.64	0.64	0.25
ET	0.51	68.47	67.59	68.04	0.75	0.36	70.97	54.17	63.64	0.67	0.25

Negatively_Corr_5_performance_metrics											
		Training					Validation				
Name	Thresh	Sens	Spec	Acc	AUC	MCC	Sens	Spec	Acc	AUC	MCC
RF	0.52	63.96	62.96	63.47	0.66	0.27	58.07	54.17	56.36	0.59	0.12
LR	0.53	71.17	68.52	69.86	0.73	0.40	64.52	45.83	56.36	0.61	0.11
MLP	0.48	57.66	59.26	58.45	0.57	0.17	54.84	45.83	50.91	0.49	0.01
XGB	0.50	62.16	62.04	62.10	0.62	0.24	54.84	45.83	50.91	0.56	0.01
KN	0.60	63.06	68.52	65.75	0.65	0.32	70.97	62.50	67.27	0.62	0.34
ET	0.52	62.16	62.04	62.10	0.65	0.24	67.74	58.33	63.64	0.64	0.26

Supplementary Table 6.1: List of selected features based on RFE for positively and negatively correlated Methylated sites

Positive Methylated Sites				
RFE_25	RFE_20	RFE_15	RFE_10	RFE_5
1156	1156	1156	1156	1156
5779	5779	5779	5779	5779
15644	15644	15646	19310	19310
15646	15646	19310	62691	62691
19310	19310	62691	137612	197622
19311	62691	137612	155370	
40170	137612	150770	162118	
62691	150770	155370	184476	
137612	150771	155374	197622	
150770	155366	162118	206115	
150771	155370	184475		
155366	155374	184476		
155370	162118	190943		
155374	184475	197622		
162112	184476	206115		
162115	190943			
162118	197569			
164637	197570			
184475	197622			
184476	206115			
190943				
197569				
197570				
197622				

Negative Methylated Sites				
RFE_25	RFE_20	RFE_15	RFE_10	RFE_5
7575	9374	9374	24639	24639
7577	24476	24639	24640	24640
9374	24639	24640	36304	54573
17680	24640	36304	36305	75317
24476	24642	36305	54573	75318
24632	35411	54573	75317	
24639	35412	180703	75318	
24640	36304	75317	75321	
24643	36305	75318	180703	
35411	54573	75321	180704	
35412	58323	75322		
36304	75317	99171		
36305	75318	99172		
41490	75321	180703		
41491	75322	180704		
54571	99171			
54573	99172			
58323	180703			
75317	180704			
75318	203525			
126872				
126873				
180703				
180704				

206115				
--------	--	--	--	--

203525				
--------	--	--	--	--

Supplementary Table 6.2: ML Performance of RFE selected feature sets for positively and negatively correlated Methylated sites

RFE_positively_Corr_25_performance_metrics

Model ID	Training											Validation						
	Thr	TPR	FPR	YC	Sp	Sn	AUC	Acc	Pre	MC	K	Sp	Sn	AUC	Acc	Pre	MC	K
SVC	0.64	0.88	0.17	0.71	100.00	65.22	0.83	81.82	100.00	0.69	0.64	82.76	88.46	0.86	85.45	82.14	0.71	0.71
LR	0.40	0.88	0.21	0.68	90.48	91.30	0.91	90.91	91.30	0.82	0.82	79.31	88.46	0.84	83.64	79.31	0.68	0.67
Naive Bayes	0.00	0.88	0.14	0.75	76.19	78.26	0.77	77.27	78.26	0.54	0.54	86.21	88.46	0.87	87.27	85.19	0.75	0.75
DT	1.00	0.73	0.28	0.45	66.67	69.57	0.68	68.18	69.57	0.36	0.36	72.41	73.08	0.73	72.73	70.37	0.45	0.45
RF	0.27	0.88	0.24	0.64	76.19	73.91	0.75	75.00	77.27	0.50	0.50	75.86	88.46	0.82	81.82	76.67	0.64	0.64
ET	0.61	0.85	0.17	0.67	80.95	86.96	0.84	84.09	83.33	0.68	0.68	82.76	84.62	0.84	83.64	81.48	0.67	0.67
AdaBooSt	0.50	0.85	0.17	0.67	80.00	79.17	0.80	79.55	82.61	0.59	0.59	82.76	84.62	0.84	83.64	81.48	0.67	0.67
Gradient Boosting	0.64	0.81	0.17	0.64	85.71	86.96	0.86	86.36	86.96	0.73	0.73	82.76	80.77	0.82	81.82	80.77	0.64	0.64
MLP	0.63	0.85	0.07	0.78	90.48	91.30	0.91	90.91	91.30	0.82	0.82	93.10	84.62	0.89	89.09	91.67	0.78	0.78
XGBoost	0.25	0.88	0.28	0.61	80.95	78.26	0.80	79.55	81.82	0.59	0.59	72.41	88.46	0.80	80.00	74.19	0.61	0.60

RFE_positively_Corr_20_performance_metrics

Model ID	Training											Validation						
	Thr	TPR	FPR	YC	Sp	Sn	AUC	Acc	Pre	MC	K	Sp	Sn	AUC	Acc	Pre	MC	K
SVC	0.88	0.65	0.00	0.65	100.00	60.87	0.80	79.55	100.00	0.65	0.60	100.00	65.38	0.83	83.64	100.00	0.71	0.67
LR	0.34	0.88	0.21	0.68	85.71	86.96	0.86	86.36	86.96	0.73	0.73	79.31	88.46	0.84	83.64	79.31	0.68	0.67
Naive	0.00	0.88	0.07	0.82	85.71	78.26	0.82	81.82	85.71	0.64	0.64	93.10	88.46	0.91	90.91	92.00	0.82	0.82

Bayes																			
DT	1.00	0.77	0.17	0.60	80.00	73.91	0.77	76.74	80.95	0.54	0.54	82.76	76.92	0.80	80.00	80.00	0.60	0.60	
RF	0.65	0.81	0.14	0.67	75.00	73.91	0.74	74.42	77.27	0.49	0.49	86.21	80.77	0.83	83.64	84.00	0.67	0.67	
ET	0.31	0.92	0.24	0.68	80.95	82.61	0.82	81.82	82.61	0.64	0.64	75.86	92.31	0.84	83.64	77.42	0.69	0.68	
AdaBooSt	0.54	0.85	0.21	0.64	85.71	91.30	0.89	88.64	87.50	0.77	0.77	79.31	84.62	0.82	81.82	78.57	0.64	0.64	
Gradient Boosting	0.66	0.77	0.14	0.63	76.19	73.91	0.75	75.00	77.27	0.50	0.50	86.21	76.92	0.82	81.82	83.33	0.64	0.63	
MLP	0.19	0.88	0.21	0.68	90.48	91.30	0.91	90.91	91.30	0.82	0.82	79.31	88.46	0.84	83.64	79.31	0.68	0.67	
XGBoost	0.85	0.73	0.07	0.66	80.00	73.91	0.77	76.74	80.95	0.54	0.54	93.10	73.08	0.83	83.64	90.48	0.68	0.67	

RFE_positively_Corr_15_performance_metrics

	Training											Validation						
Model ID	Thr	TPR	FPR	YC	Sp	Sn	AUC	Acc	Pre	MC	K	Sp	Sn	AUC	Acc	Pre	MC	K
SVC	0.22	0.92	0.21	0.72	100.00	78.26	0.89	88.64	100.00	0.80	0.77	79.31	92.31	0.86	85.45	80.00	0.72	0.71
LR	0.29	0.92	0.21	0.72	90.48	91.30	0.91	90.91	91.30	0.82	0.82	79.31	92.31	0.86	85.45	80.00	0.72	0.71
Naive Bayes	0.00	0.92	0.21	0.72	80.95	91.30	0.86	86.36	84.00	0.73	0.73	79.31	92.31	0.86	85.45	80.00	0.72	0.71
DT	1.00	0.81	0.14	0.67	85.71	86.96	0.86	86.36	86.96	0.73	0.73	86.21	80.77	0.83	83.64	84.00	0.67	0.67
RF	0.41	0.88	0.14	0.75	80.95	82.61	0.82	81.82	82.61	0.64	0.64	86.21	88.46	0.87	87.27	85.19	0.75	0.75
ET	0.28	0.88	0.14	0.75	90.48	86.96	0.89	88.64	90.91	0.77	0.77	86.21	88.46	0.87	87.27	85.19	0.75	0.75
AdaBooSt	0.66	0.69	0.03	0.66	76.19	78.26	0.77	77.27	78.26	0.54	0.54	96.55	69.23	0.83	83.64	94.74	0.69	0.67
Gradient Boosting	0.15	0.85	0.21	0.64	85.71	82.61	0.84	84.09	86.36	0.68	0.68	79.31	84.62	0.82	81.82	78.57	0.64	0.64
MLP	0.25	0.92	0.21	0.72	90.48	86.96	0.89	88.64	90.91	0.77	0.77	79.31	92.31	0.86	85.45	80.00	0.72	0.71
XGBoost	0.17	0.85	0.17	0.67	66.67	69.57	0.68	68.18	69.57	0.36	0.36	82.76	84.62	0.84	83.64	81.48	0.67	0.67

RFE_positively_Corr_10_performance_metrics

					Training							Validation						
Model ID	Thr	TPR	FPR	YC	Sp	Sn	AUC	Acc	Pre	MC	K	Sp	Sn	AUC	Acc	Pre	MC	K
SVC	0.36	0.81	0.14	0.67	100.00	69.57	0.85	84.09	100.00	0.72	0.69	86.21	80.77	0.83	83.64	84.00	0.67	0.67
LR	0.42	0.81	0.14	0.67	90.48	91.30	0.91	90.91	91.30	0.82	0.82	86.21	80.77	0.83	83.64	84.00	0.67	0.67
Naive Bayes	0.00	0.81	0.14	0.67	90.48	82.61	0.87	86.36	90.48	0.73	0.73	86.21	80.77	0.83	83.64	84.00	0.67	0.67
DT	1.00	0.65	0.14	0.52	90.48	86.96	0.89	88.64	90.91	0.77	0.77	86.21	65.38	0.76	76.36	80.95	0.53	0.52
RF	0.38	0.81	0.14	0.67	90.48	86.96	0.89	88.64	90.91	0.77	0.77	86.21	80.77	0.83	83.64	84.00	0.67	0.67
ET	0.33	0.81	0.14	0.67	90.48	86.96	0.89	88.64	90.91	0.77	0.77	86.21	80.77	0.83	83.64	84.00	0.67	0.67
AdaBooSt	0.52	0.77	0.14	0.63	90.48	91.30	0.91	90.91	91.30	0.82	0.82	86.21	76.92	0.82	81.82	83.33	0.64	0.63
Gradient Boosting	0.22	0.77	0.14	0.63	90.48	91.30	0.91	90.91	91.30	0.82	0.82	86.21	76.92	0.82	81.82	83.33	0.64	0.63
MLP	0.54	0.81	0.14	0.67	90.48	91.30	0.91	90.91	91.30	0.82	0.82	86.21	80.77	0.83	83.64	84.00	0.67	0.67
XGBoost	0.44	0.81	0.14	0.67	90.48	91.30	0.91	90.91	91.30	0.82	0.82	86.21	80.77	0.83	83.64	84.00	0.67	0.67

RFE_positively_Corr_5_performance_metrics

					Training							Validation						
Model ID	Thr	TPR	FPR	YC	Sp	Sn	AUC	Acc	Pre	MC	K	Sp	Sn	AUC	Acc	Pre	MC	K
SVC	0.82	0.69	0.10	0.59	95.24	56.52	0.76	75.00	92.86	0.56	0.51	89.66	69.23	0.79	80.00	85.71	0.61	0.59
LR	0.73	0.69	0.07	0.62	95.24	73.91	0.85	84.09	94.44	0.70	0.68	93.10	69.23	0.81	81.82	90.00	0.65	0.63
Naive Bayes	1.00	0.69	0.07	0.62	95.24	69.57	0.82	81.82	94.12	0.66	0.64	93.10	69.23	0.81	81.82	90.00	0.65	0.63
DT	1.00	0.65	0.10	0.55	95.24	73.91	0.85	84.09	94.44	0.70	0.68	89.66	65.38	0.78	78.18	85.00	0.57	0.56
RF	0.93	0.69	0.10	0.59	95.24	73.91	0.85	84.09	94.44	0.70	0.68	89.66	69.23	0.79	80.00	85.71	0.61	0.59
ET	0.91	0.69	0.10	0.59	95.24	73.91	0.85	84.09	94.44	0.70	0.68	89.66	69.23	0.79	80.00	85.71	0.61	0.59
AdaBooSt	0.60	0.69	0.07	0.62	95.24	73.91	0.85	84.09	94.44	0.70	0.68	93.10	69.23	0.81	81.82	90.00	0.65	0.63
Gradient Boosting	0.71	0.69	0.10	0.59	95.24	73.91	0.85	84.09	94.44	0.70	0.68	89.66	69.23	0.79	80.00	85.71	0.61	0.59

MLP	0.84	0.69	0.07	0.62	95.24	73.91	0.85	84.09	94.44	0.70	0.68	93.10	69.23	0.81	81.82	90.00	0.65	0.63
XGBoost	0.81	0.69	0.10	0.59	95.24	73.91	0.85	84.09	94.44	0.70	0.68	89.66	69.23	0.79	80.00	85.71	0.61	0.59

RFE_negatively_Corr_25_performance_metrics

Model ID	Thr	TPR	FPR	YC	Training							Validation						
					Sp	Sn	AUC	Acc	Pre	MC	K	Sp	Sn	AUC	Acc	Pre	MC	K
SVC	0.36	0.92	0.52	0.41	66.67	65.22	0.66	65.91	68.18	0.32	0.32	48.28	92.31	0.70	69.09	61.54	0.45	0.40
LR	0.29	0.96	0.79	0.17	57.14	52.17	0.55	54.55	57.14	0.09	0.09	20.69	96.15	0.58	56.36	52.08	0.25	0.16
Naive Bayes	0.00	0.96	0.52	0.44	75.00	73.91	0.74	74.42	77.27	0.49	0.49	48.28	96.15	0.72	70.91	62.50	0.50	0.43
DT	1.00	0.50	0.45	0.05	66.67	65.22	0.66	65.91	68.18	0.32	0.32	55.17	50.00	0.53	52.73	50.00	0.05	0.05
RF	0.51	0.85	0.34	0.50	61.90	73.91	0.68	68.18	68.00	0.36	0.36	65.52	84.62	0.75	74.55	68.75	0.51	0.50
ET	0.53	0.81	0.24	0.57	65.00	69.57	0.67	67.44	69.57	0.35	0.35	75.86	80.77	0.78	78.18	75.00	0.57	0.56
AdaBooSt	0.50	0.81	0.34	0.46	61.90	65.22	0.64	63.64	65.22	0.27	0.27	65.52	80.77	0.73	72.73	67.74	0.47	0.46
Gradient Boosting	0.36	0.85	0.28	0.57	71.43	69.57	0.71	70.45	72.73	0.41	0.41	72.41	84.62	0.79	78.18	73.33	0.57	0.57
MLP	0.56	0.69	0.48	0.21	57.14	60.87	0.59	59.09	60.87	0.18	0.18	51.72	69.23	0.60	60.00	56.25	0.21	0.21
XGBoost	0.45	0.85	0.28	0.57	70.00	69.57	0.70	69.77	72.73	0.39	0.39	72.41	84.62	0.79	78.18	73.33	0.57	0.57

RFE_negatively_Corr_20_performance_metrics

Model ID	Thr	TPR	FPR	YC	Training							Validation						
					Sp	Sn	AUC	Acc	Pre	MC	K	Sp	Sn	AUC	Acc	Pre	MC	K
SVC	0.42	0.88	0.52	0.37	61.90	60.87	0.61	61.36	63.64	0.23	0.23	48.28	88.46	0.68	67.27	60.53	0.40	0.36
LR	0.17	0.96	0.83	0.13	61.90	52.17	0.57	56.82	60.00	0.14	0.14	17.24	96.15	0.57	54.55	51.02	0.21	0.13
Naive Bayes	0.15	0.81	0.41	0.39	75.00	73.91	0.74	74.42	77.27	0.49	0.49	58.62	80.77	0.70	69.09	63.64	0.40	0.39
DT	1.00	0.69	0.38	0.31	70.00	69.57	0.70	69.77	72.73	0.39	0.39	62.07	69.23	0.66	65.45	62.07	0.31	0.31

RF	0.62	0.73	0.17	0.56	71.43	73.91	0.73	72.73	73.91	0.45	0.45	82.76	73.08	0.78	78.18	79.17	0.56	0.56
ET	0.47	0.92	0.45	0.47	70.00	65.22	0.68	67.44	71.43	0.35	0.35	55.17	92.31	0.74	72.73	64.86	0.51	0.46
AdaBooSt	0.50	0.73	0.34	0.39	60.00	60.87	0.60	60.47	63.64	0.21	0.21	65.52	73.08	0.69	69.09	65.52	0.39	0.38
Gradient Boosting	0.87	0.62	0.10	0.51	61.90	60.87	0.61	61.36	63.64	0.23	0.23	89.66	61.54	0.76	76.36	84.21	0.54	0.52
MLP	0.16	0.96	0.62	0.34	70.00	66.67	0.68	68.18	72.73	0.37	0.36	37.93	96.15	0.67	65.45	58.14	0.41	0.33
XGBoost	0.60	0.73	0.24	0.49	60.00	60.87	0.60	60.47	63.64	0.21	0.21	75.86	73.08	0.74	74.55	73.08	0.49	0.49

RFE_negatively_Corr_15_performance_metrics

	Training											Validation						
Model ID	Thr	TPR	FPR	YC	Sp	Sn	AUC	Acc	Pre	MC	K	Sp	Sn	AUC	Acc	Pre	MC	K
SVC	0.49	0.73	0.34	0.39	61.90	82.61	0.72	72.73	70.37	0.46	0.45	65.52	73.08	0.69	69.09	65.52	0.39	0.38
LR	0.59	0.35	0.28	0.07	65.00	58.33	0.62	61.36	66.67	0.23	0.23	72.41	34.62	0.54	54.55	52.94	0.08	0.07
Naive Bayes	0.76	0.77	0.34	0.42	80.00	73.91	0.77	76.74	80.95	0.54	0.54	65.52	76.92	0.71	70.91	66.67	0.43	0.42
DT	1.00	0.62	0.45	0.17	57.14	65.22	0.61	61.36	62.50	0.22	0.22	55.17	61.54	0.58	58.18	55.17	0.17	0.17
RF	0.46	0.92	0.48	0.44	57.14	56.52	0.57	56.82	59.09	0.14	0.14	51.72	92.31	0.72	70.91	63.16	0.48	0.43
ET	0.44	0.88	0.45	0.44	60.00	60.87	0.60	60.47	63.64	0.21	0.21	55.17	88.46	0.72	70.91	63.89	0.46	0.43
AdaBooSt	0.49	0.85	0.48	0.36	60.00	60.87	0.60	60.47	63.64	0.21	0.21	51.72	84.62	0.68	67.27	61.11	0.38	0.36
Gradient Boosting	0.41	0.92	0.48	0.44	60.00	56.52	0.58	58.14	61.90	0.16	0.16	51.72	92.31	0.72	70.91	63.16	0.48	0.43
MLP	0.57	0.46	0.28	0.19	50.00	54.17	0.52	52.27	56.52	0.04	0.04	72.41	46.15	0.59	60.00	60.00	0.19	0.19
XGBoost	0.24	0.85	0.45	0.40	61.90	65.22	0.64	63.64	65.22	0.27	0.27	55.17	84.62	0.70	69.09	62.86	0.41	0.39

RFE_negatively_Corr_10_performance_metrics

	Training											Validation						
Model ID	Thr	TPR	FPR	YC	Sp	Sn	AUC	Acc	Pre	MC	K	Sp	Sn	AUC	Acc	Pre	MC	K

SVC	0.61	0.65	0.28	0.38	61.90	82.61	0.72	72.73	70.37	0.46	0.45	72.41	65.38	0.69	69.09	68.00	0.38	0.38
LR	0.39	0.77	0.62	0.15	61.90	69.57	0.66	65.91	66.67	0.32	0.32	37.93	76.92	0.57	56.36	52.63	0.16	0.15
Naive Bayes	0.75	0.73	0.31	0.42	75.00	69.57	0.72	72.09	76.19	0.44	0.44	68.97	73.08	0.71	70.91	67.86	0.42	0.42
DT	1.00	0.62	0.41	0.20	66.67	65.22	0.66	65.91	68.18	0.32	0.32	58.62	61.54	0.60	60.00	57.14	0.20	0.20
RF	0.42	0.88	0.38	0.51	65.00	60.87	0.63	62.79	66.67	0.26	0.26	62.07	88.46	0.75	74.55	67.65	0.52	0.50
ET	0.61	0.65	0.17	0.48	61.90	65.22	0.64	63.64	65.22	0.27	0.27	82.76	65.38	0.74	74.55	77.27	0.49	0.49
AdaBooSt	0.49	0.92	0.45	0.47	71.43	65.22	0.68	68.18	71.43	0.37	0.36	55.17	92.31	0.74	72.73	64.86	0.51	0.46
Gradient Boosting	0.40	0.88	0.34	0.54	61.90	60.87	0.61	61.36	63.64	0.23	0.23	65.52	88.46	0.77	76.36	69.70	0.55	0.53
MLP	0.34	0.73	0.62	0.11	60.00	58.33	0.59	59.09	63.64	0.18	0.18	37.93	73.08	0.56	54.55	51.35	0.12	0.11
XGBoost	0.66	0.69	0.24	0.45	61.90	52.17	0.57	56.82	60.00	0.14	0.14	75.86	69.23	0.73	72.73	72.00	0.45	0.45

RFE_negatively_Corr_5_performance_metrics

Model ID	Training											Validation						
	Thr	TPR	FPR	YC	Sp	Sn	AUC	Acc	Pre	MC	K	Sp	Sn	AUC	Acc	Pre	MC	K
SVC	0.45	0.81	0.38	0.43	65.00	73.91	0.69	69.77	70.83	0.39	0.39	62.07	80.77	0.71	70.91	65.63	0.43	0.42
LR	0.49	0.77	0.38	0.39	71.43	78.26	0.75	75.00	75.00	0.50	0.50	62.07	76.92	0.70	69.09	64.52	0.39	0.39
Naive Bayes	0.52	0.77	0.38	0.39	70.00	78.26	0.74	74.42	75.00	0.48	0.48	62.07	76.92	0.70	69.09	64.52	0.39	0.39
DT	1.00	0.58	0.52	0.06	65.00	65.22	0.65	65.12	68.18	0.30	0.30	48.28	57.69	0.53	52.73	50.00	0.06	0.06
RF	0.47	0.81	0.48	0.32	71.43	69.57	0.71	70.45	72.73	0.41	0.41	51.72	80.77	0.66	65.45	60.00	0.34	0.32
ET	0.57	0.73	0.28	0.45	71.43	73.91	0.73	72.73	73.91	0.45	0.45	72.41	73.08	0.73	72.73	70.37	0.45	0.45
AdaBooSt	0.50	0.85	0.48	0.36	70.00	60.87	0.65	65.12	70.00	0.31	0.31	51.72	84.62	0.68	67.27	61.11	0.38	0.36
Gradient Boosting	0.60	0.69	0.41	0.28	76.19	78.26	0.77	77.27	78.26	0.54	0.54	58.62	69.23	0.64	63.64	60.00	0.28	0.28
MLP	0.48	0.58	0.41	0.16	61.90	69.57	0.66	65.91	66.67	0.32	0.32	58.62	57.69	0.58	58.18	55.56	0.16	0.16

XGBoost	0.05	1.00	0.76	0.24	61.90	60.87	0.61	61.36	63.64	0.23	0.23	24.14	100.0	0.62	60.00	54.17	0.36	0.23
----------------	------	------	------	------	-------	-------	------	-------	-------	------	------	-------	-------	------	-------	-------	------	------

#Thr: Threshold; YC: Youden Coeff; Sp: Specificity; Sn: Sensitivity; Acc: Accuracy; Pre: Precision; MC: Mathews Coeff; K :Kappa

Supplementary Table 7.1: List of selected features based on SFS for positively and negatively correlated Methylated sites

SFS_10_Pos_Met_sites	SFS_4_Neg_Met_sites
5779	17680
19311	75319
33055	100953
62691	116025
93487	
155374	
162112	
181490	
181491	
190944	

Supplementary Table 7.2: ML performance of selected features based on SFS for positively and negatively correlated Methylated sites

SFS_Positively_Top_10 correlated MS using SFS																		
Model ID	Thr	TPR	FPR	YC	Training							Validation						
					Sp	Sn	AUC	Acc	Pre	MC	K	Sp	Sn	AUC	Acc	Pre	MC	K
SVC	0.56	0.77	0.24	0.53	80.95	78.26	0.80	79.55	81.82	0.59	0.59	75.86	76.92	0.76	76.36	74.07	0.53	0.53
LR	0.65	0.81	0.10	0.70	76.19	73.91	0.75	75.00	77.27	0.50	0.50	89.66	80.77	0.85	85.45	87.50	0.71	0.71
Naive Bayes	1.00	0.77	0.14	0.63	71.43	73.91	0.73	72.73	73.91	0.45	0.45	86.21	76.92	0.82	81.82	83.33	0.64	0.63

DT	1.00	0.85	0.21	0.64	80.95	91.30	0.86	86.36	84.00	0.73	0.73	79.31	84.62	0.82	81.82	78.57	0.64	0.64
RF	0.46	0.85	0.28	0.57	95.24	82.61	0.89	88.64	95.00	0.78	0.77	72.41	84.62	0.79	78.18	73.33	0.57	0.57
ET	0.76	0.77	0.10	0.67	80.95	86.96	0.84	84.09	83.33	0.68	0.68	89.66	76.92	0.83	83.64	86.96	0.67	0.67
AdaBooSt	0.51	0.77	0.24	0.53	76.19	78.26	0.77	77.27	78.26	0.54	0.54	75.86	76.92	0.76	76.36	74.07	0.53	0.53
Gradient Boosting	0.89	0.69	0.07	0.62	80.95	86.96	0.84	84.09	83.33	0.68	0.68	93.10	69.23	0.81	81.82	90.00	0.65	0.63
MLP	0.79	0.73	0.07	0.66	76.19	78.26	0.77	77.27	78.26	0.54	0.54	93.10	73.08	0.83	83.64	90.48	0.68	0.67
XGBoost	0.81	0.73	0.14	0.59	80.95	82.61	0.82	81.82	82.61	0.64	0.64	86.21	73.08	0.80	80.00	82.61	0.60	0.60

SFS_Negatively_Top 4 correlated MS using SFS

	Training											Validation						
Model ID	Thr	TPR	FPR	YC	Sp	Sn	AUC	Acc	Pre	MC	K	Sp	Sn	AUC	Acc	Pre	MC	K
SVC	0.62	0.77	0.24	0.53	75.00	82.61	0.79	79.07	79.17	0.58	0.58	75.86	76.92	0.76	76.36	74.07	0.53	0.53
LR	0.48	0.81	0.38	0.43	71.43	73.91	0.73	72.73	73.91	0.45	0.45	62.07	80.77	0.71	70.91	65.63	0.43	0.42
Naive Bayes	0.70	0.81	0.34	0.46	80.00	86.96	0.83	83.72	83.33	0.67	0.67	65.52	80.77	0.73	72.73	67.74	0.47	0.46
DT	1.00	0.77	0.72	0.05	66.67	69.57	0.68	68.18	69.57	0.36	0.36	27.59	76.92	0.52	50.91	48.78	0.05	0.04
RF	0.83	0.31	0.14	0.17	61.90	73.91	0.68	68.18	68.00	0.36	0.36	86.21	30.77	0.58	60.00	66.67	0.21	0.17
ET	0.57	0.73	0.31	0.42	66.67	78.26	0.72	72.73	72.00	0.45	0.45	68.97	73.08	0.71	70.91	67.86	0.42	0.42
AdaBooSt	0.50	0.85	0.59	0.26	76.19	78.26	0.77	77.27	78.26	0.54	0.54	41.38	84.62	0.63	61.82	56.41	0.29	0.25
Gradient Boosting	0.46	0.77	0.48	0.29	57.14	60.87	0.59	59.09	60.87	0.18	0.18	51.72	76.92	0.64	63.64	58.82	0.29	0.28
MLP	0.47	0.81	0.72	0.08	55.00	58.33	0.57	56.82	60.87	0.13	0.13	27.59	80.77	0.54	52.73	50.00	0.10	0.08
XGBoost	0.99	0.27	0.10	0.17	61.90	60.87	0.61	61.36	63.64	0.23	0.23	89.66	26.92	0.58	60.00	70.00	0.21	0.17

Supplementary Table 8.1: List of selected features based on SVC-L1 for positively and negatively correlated Methylated sites

SVC-L1_9_Pos_Met_sites		SVC-L1_50_Neg_Met_sites				
33055		3658	54572	125191	24476	89080
93487		7573	54573	149453	24632	90817
14879		7574	57404	171893	24643	90819
22039		7575	58323	180704	30581	99173
32433		7699	75129	189312	35411	100954
38139		7703	75317	189313	35412	100957
86829		9376	75319	202309	36303	113054
181489		17680	75322	202310	36304	114431
196742		17992	78188	203525	36305	116026
		18002	84787	204581	41490	123336

Supplementary Table 8.2: ML performance of selected features based on SVC-L1 for positively and negatively correlated Methylated sites

Top 9 positively correlated MS using SVC-L1																		
	Training											Validation						
Model ID	Thr	TPR	FPR	YC	Sp	Sn	AUC	Acc	Pre	MC	K	Sp	Sn	AUC	Acc	Pre	MC	K
SVC	0.78	0.65	0.07	0.58	85.71	78.26	0.82	81.82	85.71	0.64	0.64	93.10	65.38	0.79	80.00	89.47	0.61	0.59
LR	0.73	0.69	0.03	0.66	76.19	73.91	0.75	75.00	77.27	0.50	0.50	96.55	69.23	0.83	83.64	94.74	0.69	0.67
Naive Bayes	0.00	0.88	0.24	0.64	95.24	60.87	0.78	77.27	93.33	0.59	0.55	75.86	88.46	0.82	81.82	76.67	0.64	0.64
DT	1.00	0.81	0.34	0.46	90.48	86.96	0.89	88.64	90.91	0.77	0.77	65.52	80.77	0.73	72.73	67.74	0.47	0.46
RF	0.38	0.88	0.34	0.54	75.00	65.22	0.70	69.77	75.00	0.40	0.40	65.52	88.46	0.77	76.36	69.70	0.55	0.53

ET	0.57	0.81	0.24	0.57	66.67	65.22	0.66	65.91	68.18	0.32	0.32	75.86	80.77	0.78	78.18	75.00	0.57	0.56
AdaBooSt	0.51	0.88	0.14	0.75	71.43	69.57	0.71	70.45	72.73	0.41	0.41	86.21	88.46	0.87	87.27	85.19	0.75	0.75
Gradient Boosting	0.62	0.85	0.28	0.57	80.95	86.96	0.84	84.09	83.33	0.68	0.68	72.41	84.62	0.79	78.18	73.33	0.57	0.57
MLP	0.61	0.77	0.17	0.60	66.67	65.22	0.66	65.91	68.18	0.32	0.32	82.76	76.92	0.80	80.00	80.00	0.60	0.60
XGBoost	0.89	0.73	0.24	0.49	76.19	86.96	0.82	81.82	80.00	0.64	0.63	75.86	73.08	0.74	74.55	73.08	0.49	0.49

Top 50 negatively correlated MS using SVC-L1

	Training											Validation						
Model ID	Thr	TPR	FPR	YC	Sp	Sn	AUC	Acc	Pre	MC	K	Sp	Sn	AUC	Acc	Pre	MC	K
SVC	0.40	0.85	0.48	0.36	71.43	65.22	0.68	68.18	71.43	0.37	0.36	51.72	84.62	0.68	67.27	61.11	0.38	0.36
LR	0.33	0.88	0.59	0.30	65.00	60.87	0.63	62.79	66.67	0.26	0.26	41.38	88.46	0.65	63.64	57.50	0.33	0.29
Naive Bayes	0.00	0.92	0.45	0.47	75.00	73.91	0.74	74.42	77.27	0.49	0.49	55.17	92.31	0.74	72.73	64.86	0.51	0.46
DT	1.00	0.77	0.38	0.39	61.90	56.52	0.59	59.09	61.90	0.18	0.18	62.07	76.92	0.70	69.09	64.52	0.39	0.39
RF	0.55	0.69	0.14	0.55	71.43	69.57	0.71	70.45	72.73	0.41	0.41	86.21	69.23	0.78	78.18	81.82	0.57	0.56
ET	0.53	0.77	0.21	0.56	71.43	69.57	0.71	70.45	72.73	0.41	0.41	79.31	76.92	0.78	78.18	76.92	0.56	0.56
AdaBooSt	0.51	0.69	0.28	0.42	71.43	73.91	0.73	72.73	73.91	0.45	0.45	72.41	69.23	0.71	70.91	69.23	0.42	0.42
Gradient Boosting	0.43	0.85	0.38	0.47	71.43	78.26	0.75	75.00	75.00	0.50	0.50	62.07	84.62	0.73	72.73	66.67	0.48	0.46
MLP	0.02	0.92	0.55	0.37	50.00	50.00	0.50	50.00	54.55	0.00	0.00	44.83	92.31	0.69	67.27	60.00	0.42	0.36
XGBoost	0.37	0.92	0.34	0.58	71.43	73.91	0.73	72.73	73.91	0.45	0.45	65.52	92.31	0.79	78.18	70.59	0.59	0.57

Top 146 MS using SVC-L1 on 30971 Methylation Sites.

	Training											Validation						
Model ID	Thr	TPR	FPR	YC	Sp	Sn	AUC	Acc	Pre	MC	K	Sp	Sn	AUC	Acc	Pre	MC	K

SVC	0.63	0.59	0.32	0.27	57.14	56.52	0.57	56.82	59.09	0.14	0.14	67.86	59.26	0.64	63.64	64.00	0.27	0.27
LR	0.62	0.59	0.32	0.27	57.14	56.52	0.57	56.82	59.09	0.14	0.14	67.86	59.26	0.64	63.64	64.00	0.27	0.27
Naive Bayes	0.97	0.81	0.04	0.78	90.00	86.96	0.88	88.37	90.91	0.77	0.77	96.43	81.48	0.89	89.09	95.65	0.79	0.78
DT	1.00	0.56	0.32	0.23	71.43	69.57	0.71	70.45	72.73	0.41	0.41	67.86	55.56	0.62	61.82	62.50	0.24	0.23
RF	1.00	0.74	0.50	0.24	66.67	65.22	0.66	65.91	68.18	0.32	0.32	50.00	74.07	0.62	61.82	58.82	0.25	0.24
ET	0.58	0.67	0.11	0.56	66.67	69.57	0.68	68.18	69.57	0.36	0.36	89.29	66.67	0.78	78.18	85.71	0.58	0.56
AdaBooSt	0.55	0.67	0.11	0.56	76.19	65.22	0.71	70.45	75.00	0.42	0.41	89.29	66.67	0.78	78.18	85.71	0.58	0.56
Gradient Boosting	0.48	0.85	0.25	0.60	80.00	78.26	0.79	79.07	81.82	0.58	0.58	75.00	85.19	0.80	80.00	76.67	0.60	0.60
MLP	0.85	0.78	0.14	0.63	70.00	65.22	0.68	67.44	71.43	0.35	0.35	85.71	77.78	0.82	81.82	84.00	0.64	0.64
XGBoost	1.00	0.74	0.25	0.49	71.43	73.91	0.73	72.73	73.91	0.45	0.45	75.00	74.07	0.75	74.55	74.07	0.49	0.49
XGBoost	0.80	0.78	0.18	0.60	76.19	78.26	0.77	77.27	78.26	0.54	0.54	82.14	77.78	0.80	80.00	80.77	0.60	0.60